Liquid Exfoliation of Layered Materials

Valeria Nicolosi, Manish Chhowalla, Mercouri G. Kanatzidis, Michael S. Strano, Jonathan N. Coleman*

Background: Since at least 400 C.E., when the Mayans first used layered clays to make dyes, people have been harnessing the properties of layered materials. This gradually developed into scientific research, leading to the elucidation of the laminar structure of layered materials, detailed understanding of their properties, and eventually experiments to exfoliate or delaminate them into individual, atomically thin nanosheets. This culminated in the discovery of graphene, resulting in a new explosion of interest in two-dimensional materials.

Layered materials consist of two-dimensional platelets weakly stacked to form three-dimensional structures. The archetypal example is graphite, which consists of stacked graphene monolayers. However, there are many others: from MoS_2 and layered clays to more exotic examples such as MoO_3, GaTe, and Bi_2Se_3. These materials display a wide range of electronic, optical, mechanical, and electrochemical properties. Over the past decade, a number of methods have been developed to exfoliate layered materials in order to produce monolayer nanosheets. Such exfoliation creates extremely high-aspect-ratio nanosheets with enormous surface area, which are ideal for applications that require surface activity. More importantly, however, the two-dimensional confinement of electrons upon exfoliation leads to unprecedented optical and electrical properties.

Advances: An important advance has been the discovery that layered crystals can be exfoliated in liquids. There are a number of methods to do this that involve oxidation, ion intercalation/exchange, or surface passivation by solvents. However, all result in liquid dispersions containing large quantities of nanosheets. This brings considerable advantages: Liquid exfoliation allows the formation of thin films and composites, is potentially scaleable, and may facilitate processing by using standard technologies such as reel-to-reel manufacturing.

Although much work has focused on liquid exfoliation of graphene, such processes have also been demonstrated for a host of other materials, including MoS_2 and other related structures, layered oxides, and clays. The resultant liquid dispersions have been formed into films, hybrids, and composites for a range of applications.

Outlook: There is little doubt that the main advances are in the future. Multifunctional composites based on metal and polymer matrices will be developed that will result in enhanced mechanical, electrical, and barrier properties. Applications in energy generation and storage will abound, with layered materials appearing as electrodes or active elements in devices such as displays, solar cells, and batteries. Particularly important will be the use of MoS_2 for water splitting and metal oxides as hydrogen evolution catalysts. In addition, two-dimensional materials will find important roles in printed electronics as dielectrics, optoelectronic devices, and transistors.

To achieve this, much needs to be done. Production rates need to be increased dramatically, the degree of exfoliation improved, and methods to control nanosheet properties developed. The range of layered materials that can be exfoliated must be expanded, even as methods for chemical modification must be developed. Success in these areas will lead to a family of materials that will dominate nanomaterials science in the 21st century.

ARTICLE OUTLINE

Why Exfoliate?

Large-Scale Exfoliation in Liquids?

Pioneers

Recent Advances in Liquid Exfoliation

Potential Applications of Liquid-Exfoliated Nanosheets

Outlook

ADDITIONAL RESOURCES

Liquid exfoliation of layered crystals allows the production of suspensions of two-dimensional nanosheets, which can be formed into a range of structures. (**A**) MoS_2 powder. (**B**) WS_2 dispersed in surfactant solution. (**C**) An exfoliated MoS_2 nanosheet. (**D**) A hybrid material consisting of WS_2 nanosheets embedded in a network of carbon nanotubes.
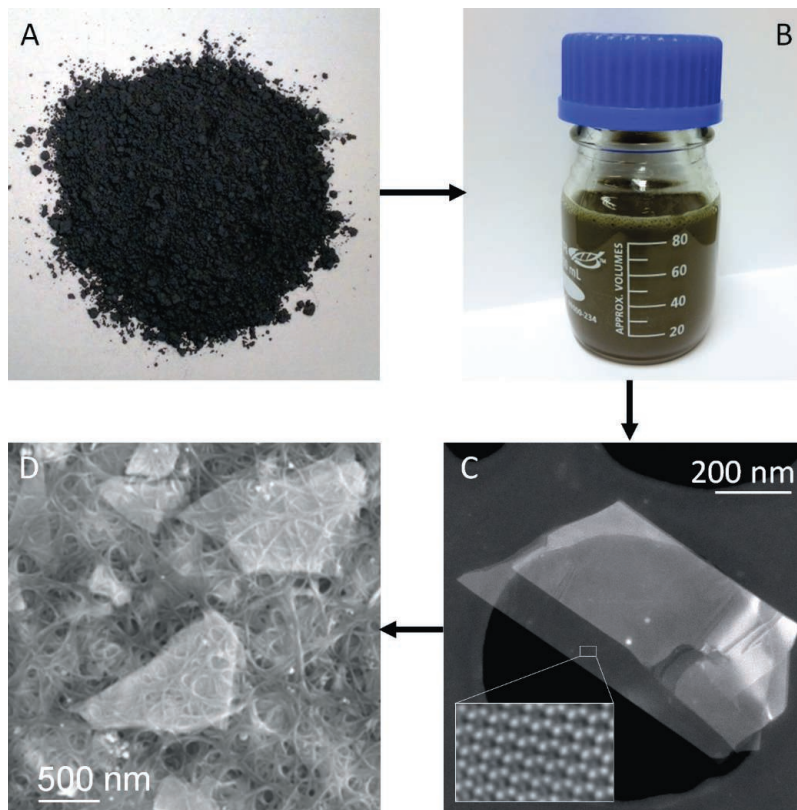
The list of author affiliations is available in the full article online.
*Corresponding author. E-mail: colemaj@tcd.ie

Liquid Exfoliation of Layered Materials

Valeria Nicolosi,[1,2] Manish Chhowalla,[3] Mercouri G. Kanatzidis,[4] Michael S. Strano,[5] Jonathan N. Coleman[1]*

Not all crystals form atomic bonds in three dimensions. Layered crystals, for instance, are those that form strong chemical bonds in-plane but display weak out-of-plane bonding. This allows them to be exfoliated into so-called nanosheets, which can be micrometers wide but less than a nanometer thick. Such exfoliation leads to materials with extraordinary values of crystal surface area, in excess of 1000 square meters per gram. This can result in dramatically enhanced surface activity, leading to important applications, such as electrodes in supercapacitors or batteries. Another result of exfoliation is quantum confinement of electrons in two dimensions, transforming the electron band structure to yield new types of electronic and magnetic materials. Exfoliated materials also have a range of applications in composites as molecularly thin barriers or as reinforcing or conductive fillers. Here, we review exfoliation—especially in the liquid phase—as a transformative process in material science, yielding new and exotic materials, which are radically different from their bulk, layered counterparts.

In 1824, Thomas H. Webb heated a mineral similar to mica and, by means of thermal exfoliation, transformed it into what is today a valuable commodity, with applications as an ion exchange resin, an insulating material, and a structural binder in cement. He named the mineral "vermiculite" for its wormlike appearance upon exfoliation (Fig. 1), from the Latin vermiculare meaning "to breed worms." Almost 200 years later, in 2004, Geim and Novosolov showed that thin transparent adhesive tape could be used to exfoliate graphite into single atomic layers of graphene and demonstrated atomically thin devices (1). As a process, exfoliation of layered solids has had a transformative effect on materials science and technology by opening up properties found in the two-dimensional (2D) exfoliated forms, not necessarily seen in their bulk counterparts.

Layered materials are defined as solids with strong in-plane chemical bonds but weak out-of-plane, van der Waals bonds. Such materials can be sheared parallel or expanded normal to the in-plane direction. In the extreme limit, these processes yield nanometer-thin—even atomically thin—sheets that are not at all characteristic of the bulk precursor. This production of extremely thin sheets from layered precursors is known as exfoliation or delamination, although in this work we will use the former term. The sheets produced are generally referred to as nanosheets, where "nano" refers to the magnitude of the thickness. Although in the ideal case such nanosheets consist of single monolayers, they are often manifested as incompletely exfoliated flakes comprising a small number (<10) of stacked monolayers.

There are many types of layered materials, which can be grouped into diverse families (Fig. 1). The simplest are the atomically thin, hexagonal sheets of graphene (1–3) and hexagonal boron nitride (h-BN) (4). Transition metal dichalcogenides (TMDs) (such as MoS_2 and WSe_2) (5, 6) and metal halides (such as PbI_2 and $MgBr_2$) (7) have near-identical structures and consist of a plane of metal atoms sandwiched between planes of halide/chalcogen atoms. Layered metal oxides (such as MnO_2, MoO_3, and $LaNb_2O_7$) (8–11) and layered double hydroxides (LDHs) [such as $Mg_6Al_2(OH)_{16}$] (8, 12) represent a diverse class of materials with a large variety of structures. Similarly, layered silicates, or clays, are minerals and exist as many different types, with well-known examples being montmorillonite or the micas (13, 14). Generally, oxides, LDH, and clay nanosheets are charged and are accompanied by charge-balancing ions (8, 14). Other interesting families are the layered III-VIs (such as InSe and GaS) (15), the layered V-VIs (such as Bi_2Te_3 and Sb_2Se_3) (16), the metal trichalcogenides, and metal trihalides. Although many other layered materials exist (Table 1), all share a planar, anisotropic bonding and therefore the potential to be exfoliated into nanosheets.

One substantial advantage of layered materials is their diversity. Even before exfoliation, the many families of layered materials display a very broad spectrum of properties. For example, TMDs (5, 6) occur as more than 40 different types depending on the combination of chalcogen (S, Se, or Te) and transition metal (5, 6). Depending on the coordination and oxidation state of the metal atoms, or doping of the lattice, TMDs can be metallic, semimetallic, or semiconducting (6). In addition, these materials display interesting electronic behavior, such as superconductivity or charge-density wave effects (6). Similarly, the many different types of layered metal oxides have interesting

electronic, electrochemical, and photonic properties (8). These materials have been fabricated into transistors, battery electrodes, and magneto-optic devices (8–10). Thus, even as bulk crystals, layered materials are an interesting and potentially useful material class. This makes them an exciting starting material for exfoliation into nanosheets. As we will see below, exfoliation dramatically enhances the range of properties displayed by an already diverse material type.

Why Exfoliate?

The simplest effect of exfoliation is to dramatically increase the accessible surface area of a material. For surface-active or catalytic materials, this can radically enhance their chemical and physical reactivity. The ion exchange ability of minerals such as vermiculite to purify water at 1000 meq/kg depends on its near-10^6-fold increase in surface area after expansion (13). In structural mechanics, the strength and stiffness of composites increase as the thickness of planar fillers, such as clay or graphite, decreases (17). When heat causes exfoliation, a layered material can be used as an intumescent (or thermally expansive) material. Hence, vermiculite and graphite are used for fire retardation in paints and firestop pillows because they reduce their density upon heating and produce an ash of low thermal conductivity.

As interest in nanotechnology has intensified in recent decades, another important advantage of exfoliation has emerged. In a layered crystal, the electronic wave function extends in three dimensions. However, after exfoliation electrons are constrained to adopt a 2D wave function, thus modifying the electronic band structure. Graphite can be transformed into a graphene monolayer after exfoliation, with electronic properties that differ greatly from any other material (1). These include an enormously high carrier mobility and other exciting properties, such as Klein tunnelling and the half-integer quantum Hall effect (1, 3). Likewise, the properties of MoS_2 depend strongly on exfoliation state. The bandgap of MoS_2 changes on exfoliation from 1.3 eV for the bulk crystal to 1.9 eV for an exfoliated nanosheet. Because the bandgap changes monotonically with number of monolayers per nanosheet, this allows the electronic response to be chosen at will (18). In addition, although multilayer MoS_2 is not photoluminescent, exfoliation-induced changes in its electronic structure lead to photoluminescent behavior in exfoliated monolayers (19). Similar behavior is expected in other layered semiconductors (5).
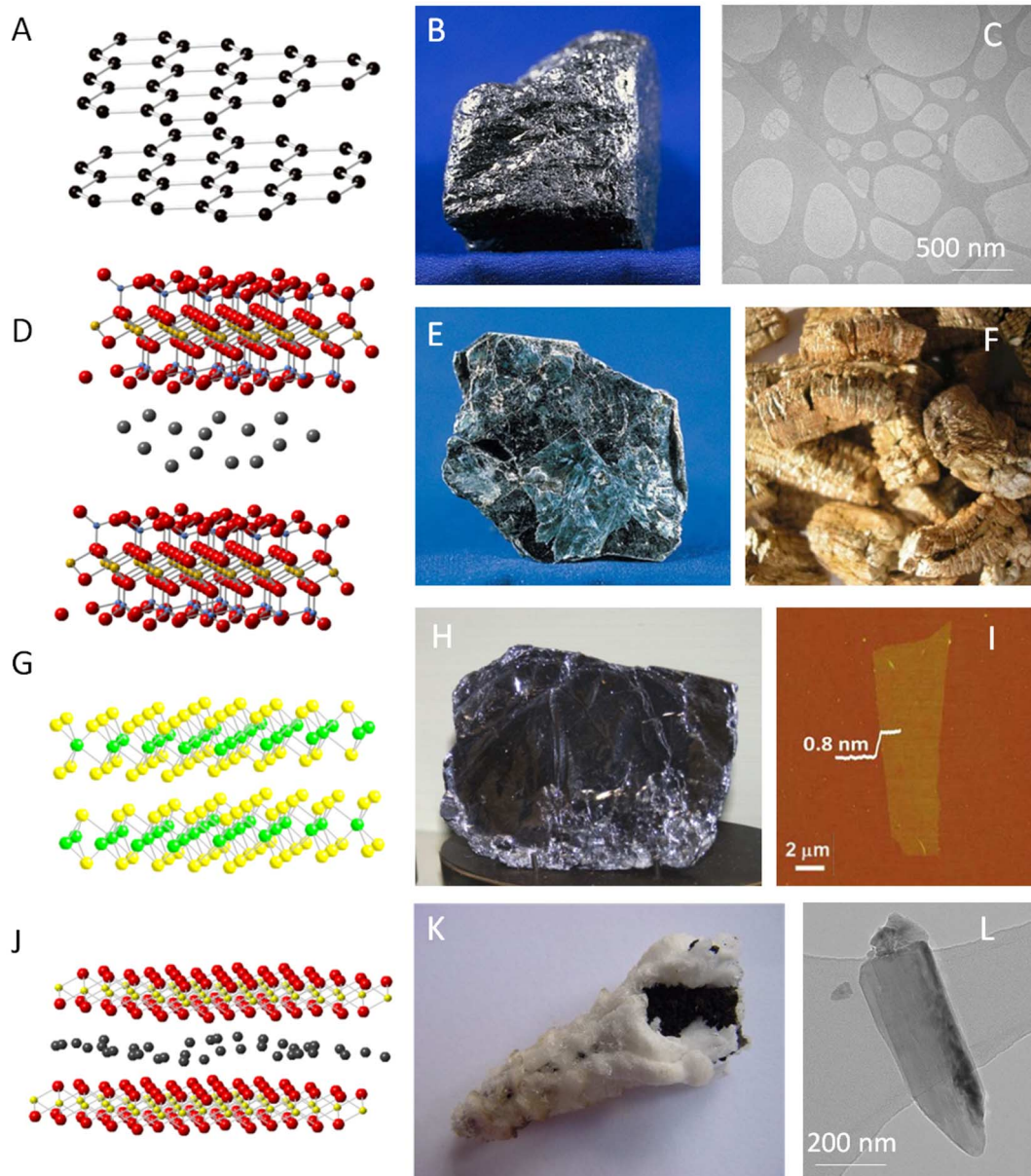
Large-Scale Exfoliation in Liquids?

The exfoliation of graphite demonstrated by Geim and Novosolov was achieved essentially by rubbing graphite on a surface (1). Such mechanical exfoliation remains the source of the highest-quality graphene samples available and has resulted in some major advances (1). However, it suffers from low yield and a production rate that is not

Fig. 1. Crystal structures, naturally occurring forms, and exfoliated products for four example layered materials. (**A**) Graphite consists of alternating stacks of hexagonally arranged carbon atoms (black spheres), (**B**) is a naturally occurring mineral, and (**C**) exfoliates to single atomic layers of carbon called graphene. (**D**) Vermiculite is a layered silicate hydrate (typically $Mg_{1.8}Fe_{0.9}Al_{4.3}SiO_{10}(OH)_2 \cdot 4(H_2O)$ that (**E**) is found naturally as a mineral and (**F**) can be exfoliated, for example, upon heating. Silicon atoms are in blue, oxygen atoms are in red, Al/Mg/Fe atoms are in yellow, and interlayer counterions are in black (H and H_2O not shown). (**G**) MoS_2 is a layered arrangement of S and Mo atoms (chalcogen atoms are in yellow, and transition metal are in green) that (**H**) is found naturally as the mineral molybdenite and (**I**) can be exfoliated to MoS_2 monolayers. (**J**) Layered manganese dioxide (manganese atoms are in yellow, oxygen is in red, and interlayer counterions are in black) occurs naturally (**K**) as birnessite and (**L**) can be exfoliated to give MnO_2 nanosheets. (C), (I), and (L) are adapted from (*48*), (*87*), and (*58*), respectively. The layer spacings for each material are graphite, 0.35 nm; vermiculite, 1.5 nm; MoS_2, 0.6 nm; and MnO_2, 0.45 nm.

technologically scalable in its current form. One possible solution is the exfoliation of layered compounds in liquids to give large quantities of dispersed nanosheets. This should allow for methods to obtain sizable quantities of 2D materials that can be processed by using existing industrial techniques, such as reel-to-reel manufacturing. Here, we briefly outline the four main liquid exfoliation techniques for layered materials (schematics are provided in Fig. 2, and examples of exfoliated nanosheets are provided in Fig. 3).

One of the oldest methods of exfoliating layered crystals with low reductive potential is oxidation and subsequent dispersion into suitable solvents. The best example is that of graphite (*20*), in which treatment with oxidizers such as sulphuric acid and potassium permanganate results in addition of hydroxyl and epoxide groups to the
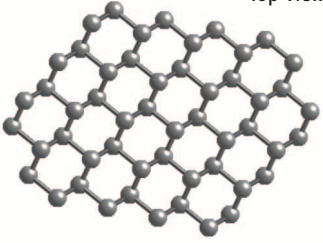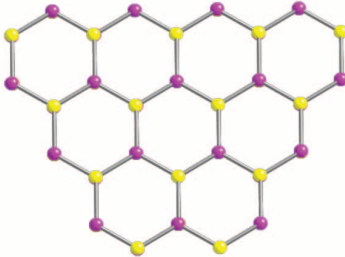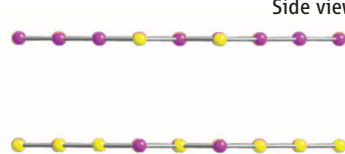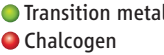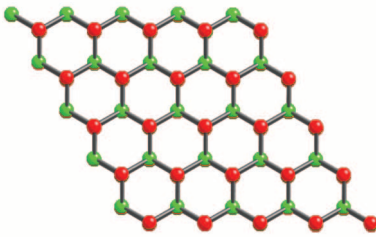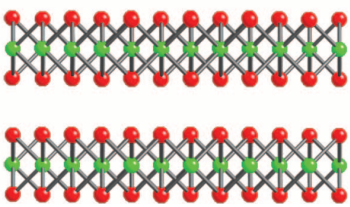
basal plane. The resulting hydrophillicity allows water intercalation and large-scale exfoliation to yield graphene oxide upon ultrasonication. The dispersed flakes are predominantly monolayers, typically hundreds of nanometers across, and stabilized against reaggregation by a negative surface charge at concentrations of up to 1 mg/ml. Dispersed graphene oxide can be chemically reduced in the liquid phase but will then aggregate unless surfactant or polymer stabilizers are present. Although reduction removes most of the oxides, structural defects remain, rendering the properties of oxidatively produced graphene substantially different from pristine graphene.
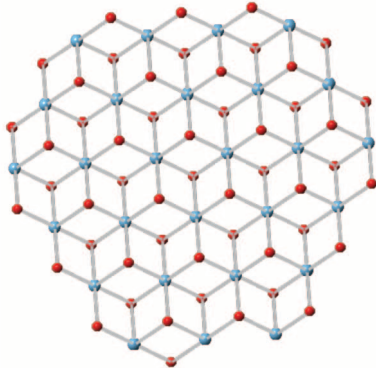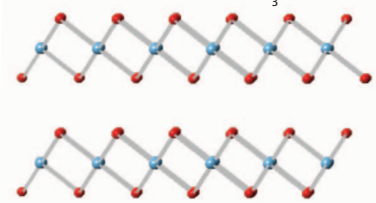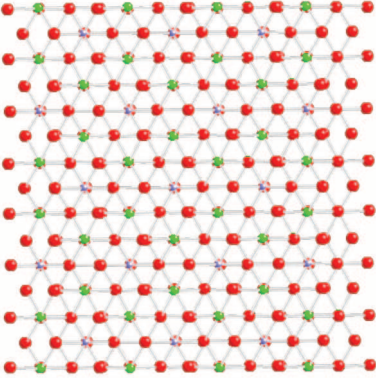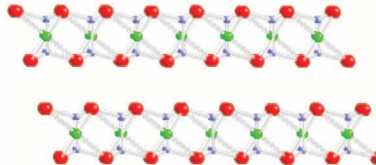
Layered materials can also strongly adsorb guest molecules into the spacing between layers, creating what are called inclusion complexes. This forms the basis of another exfoliation method that is widely applied to layered materials,
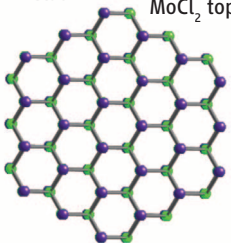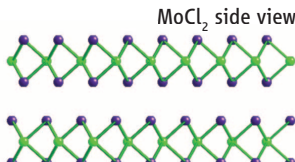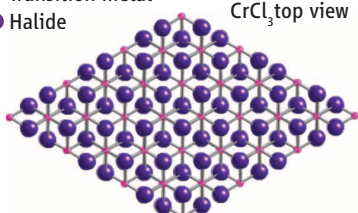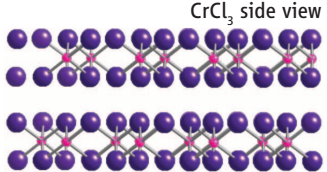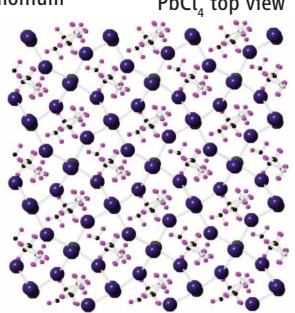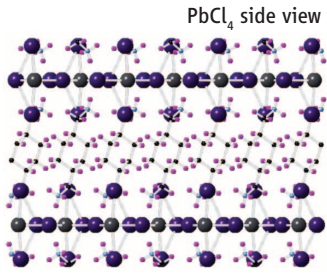
including graphite (*21*) and TMDs (*22, 23*). Intercalation, often of ionic species, increases the layer spacing, weakening the interlayer adhesion and reducing the energy barrier to exfoliation. Intercalants such as *n*-butyllithium (*22, 23*) or IBr (*21*) can transfer charge to the layers, resulting in a further reduction of interlayer binding. Subsequent treatment such as thermal shock (*21*) or ultrasonication (*22, 23*) in a liquid completes the exfoliation process. The exfoliated nanosheets can be stabilized electrostatically by a surface charge (*23*) or by surfactant addition (*21*). In the case of MoS_2, this method tends to give highly exfoliated nanosheets (*22*). However, ion intercalation–based methods have drawbacks associated with their sensitivity to ambient conditions (*22–24*).
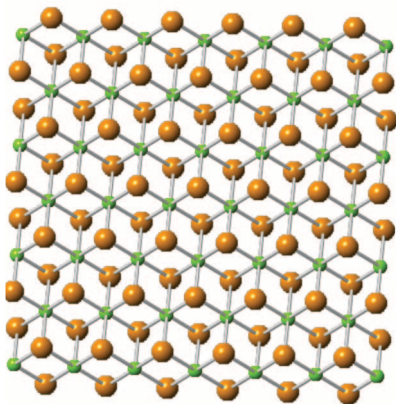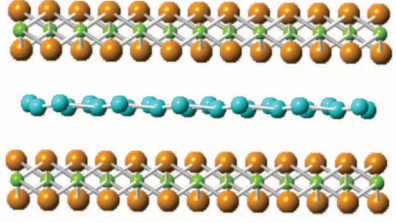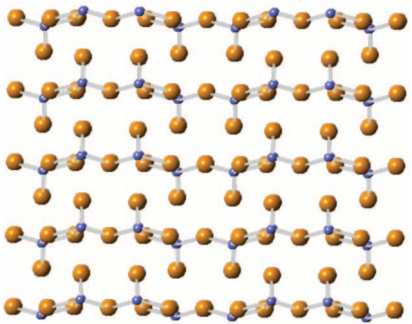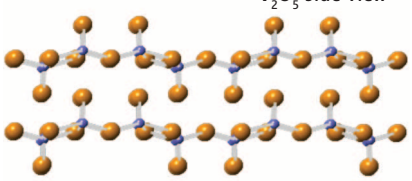
Ion exchange methods take advantage of the fact that LDHs, clays, and some metal oxides
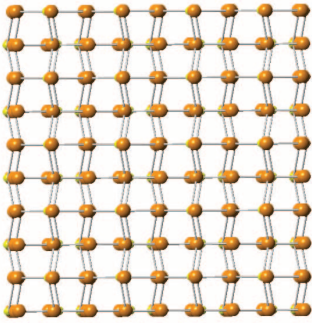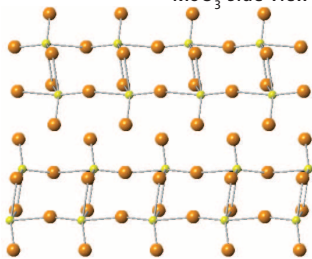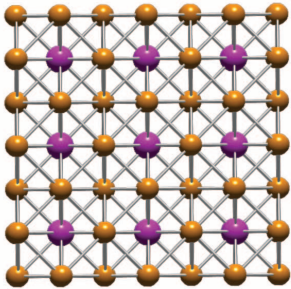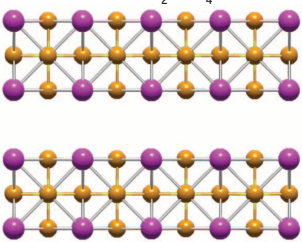
Table 1. Referenced table of families of layered compounds, including structures and information on exfoliation methods, potential applications, and availablility. This table is not exhaustive. Crystal structures were obtained from the CrystalMaker Library (www.crystalmaker.com/library/index.html).
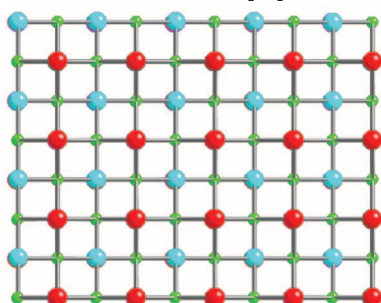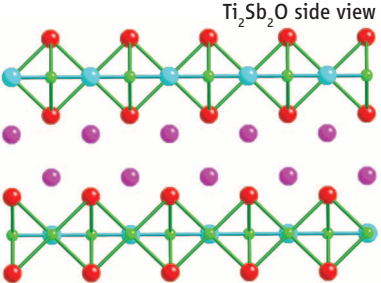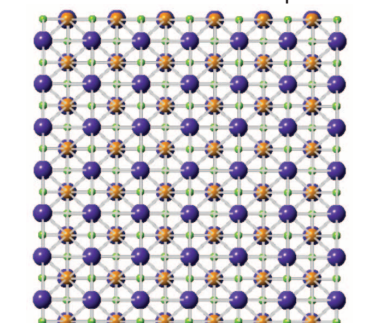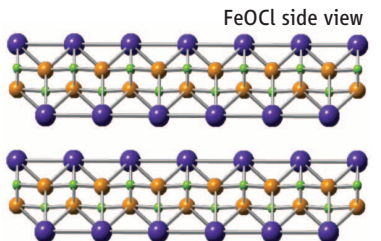
Family of layered compound	Structure	Exfoliation method	Applications	Commercial availability
Graphite	Top view / Side view	Sonication in surfactant solution (*30, 50–53*) Sonication in solvents (*27, 45–48*) Sonication in polymer solutions (*54, 55*) Graphene oxide (*20,88*)	Many (*1, 89*)	Widely available
h-BN	● Nitrogen ● Boron / Top view / Side view	Sonication in surfactant solution (*58*) Sonication in solvents (*29, 56*) Sonication in polymer solutions (*54*)	Composites (*57*) Device substrates (*90*)	Yes
Transition metal dichalcogenides (TMDs)	● Transition metal ● Chalcogen / MoS_2 top view / MoS_2 side view	Sonication in surfactant solution (*58*) Sonication in solvents (*29, 59, 60*) Sonication in polymer solutions (*54*) Ion intercalation (*91*)	Single-layer transistor (*92*) Batteries (*63, 64*) Top-gate phototransistors (*93*) Thermo-electrics (*29, 58*) Superconducting composites (*94*)	Raw materials mostly available (purity issues)
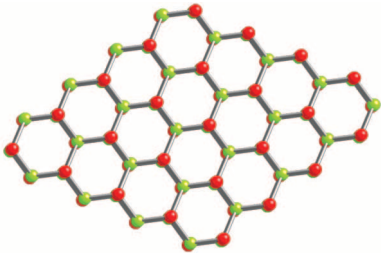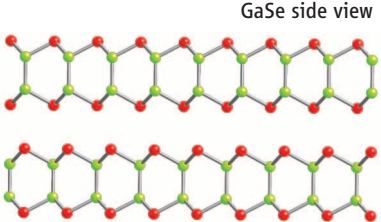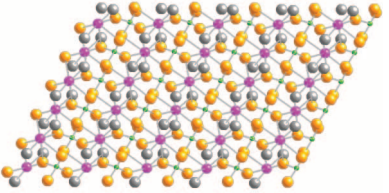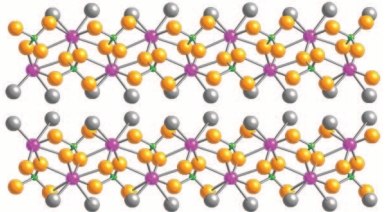
Transition metal trichalcogenides (TMDs)	AMo_3X_3, NbX_3, TiX_3, and TaX_3 (X = S, Se, or Te) 🔵 Transition metal 🔴 Chalcogen TiTe$_3$ top view TiTe$_3$ side view	Ion intercalation (*95*)	Batteries (*96*)	No, only by synthesis
	Metal phosphorous trichalcogenides (MPX_3), such as $MnPS_3$, $CdPS_3$, $NiPS_3$, $ZnPS_3$, and $Mn_{0.5}Fe_{0.5}PS_3$ 🟢 Transition metal 🔴 Chalcogen 🟣 Phosphorus MnPS$_3$ top view MnPS$_3$ side view	Intercalation (*75*)	Wide band-gap semiconductors (*97*) Magnetic properties (*98*)	No, only by synthesis
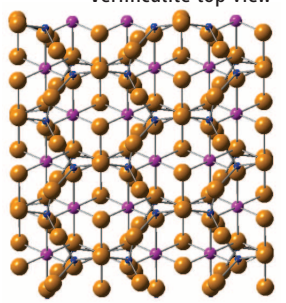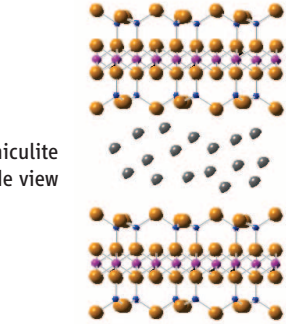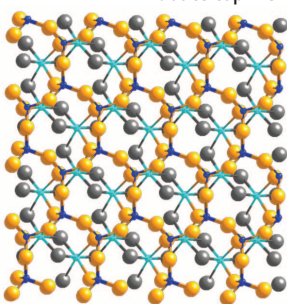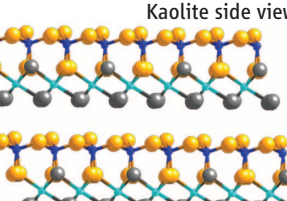
Metal halides	Transition-metal dihalides*	Ion intercalation (7) Polymer intercalation (99)		No (synthesis required)
	Metal MX_3 halides, such as $\alpha RuCl_3$, $CrCl_3$, and BiI_3†	Ion intercalation (100) Polymer intercalation (99)		No (synthesis required)
	Layer-type halides with composition MX_4, MX_5, MX_6‡	Ion intercalation (101)		No (synthesis required)
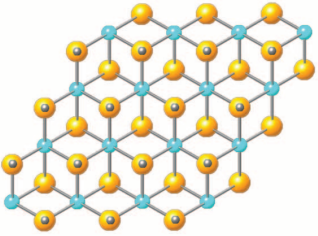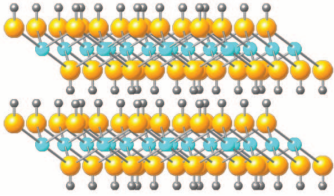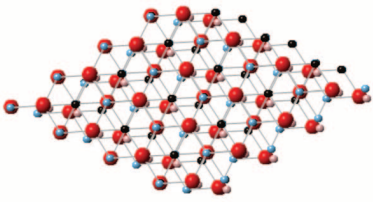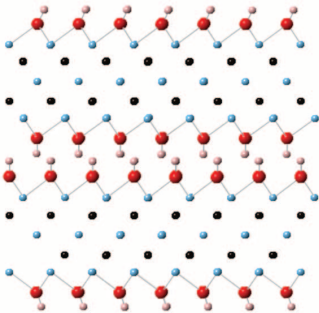
Oxides	Transition metal oxides : Ti oxides, $Ti_{0.91}O_2$, $Ti_{0.87}O_2$, Ti_3O_7, Ti_4O_9, Ti_5O_{11}; Nb oxides, Nb_3O_8, Nb_6O_{17}, HNb_3O_8;§ Mn oxides, MnO_2, Ti_3O_7, $Na_x(Mn^{4+},Mn^{3+})_2O_4$			

○ Transition metal
○ Oxygen
○ Caton

$Na_x(Mn^{4+},Mn^{3+})_2O_4$
(birnessite) top view

$Na_x(Mn^{4+},Mn^{3+})_2O_4$
(birnessite) side view

○ Vanadium
○ Oxygen

Vanadium oxide
(V_2O_5) top view

V_2O_5 side view

Ti oxides
Ion intercalation (*102*)

Mn oxides
Sonication in surfactant solution (*58*); Ion intercalation (*103*)

Nb oxides
Ion intercalation (*104*)

Va oxides
Polymer intercalation (*105*)

Supercapacitors (*106*)

Batteries (*107*)

Catalysts (*108*)

Dielectrics (*109*)

Ferroelectrics (*109*)

Some raw materials available (purity issues)

Most compounds are not available

Oxides	Trioxides, such as MoO_3, TaO_3, and hydrated WO_3 ⬤ Hydrogen ⬤ Oxygen ⚪ Transition metal MoO_3 top view MoO_3 side view	Ion intercalation (*110*) Polymer intercalation (*111*)	Electrochromics (*112*) Light emitting diodes (*113*)	Yes
	Layered trirutile phases HMWO (M = Nb, Ta), such as ($HNbWO_6$ and $HTaWO_6$)	Ion intercalation (protonation and ion exchange) (*114*)		No (only by synthesis)
	Perovskites and niobates, such as $Sr_2RuO_4 KCa_2Nb_3O_{10}$, $H_2W_2O_7$, $LaNb_2O_7$, $La_{0.90}Eu_{0.05}Nb_2O_7$, $Eu_{0.56}Ta_2O_7$, Sr_2RuO_4, $Sr_3Ru_2O_7$, $SrTa_2O_7$, $Bi_2SrTa_2O_9$, $Ca_2Nb_3O_{10}$, $Sr_2Nb_3O_{10}$, $NaCaTa_3O_{10}$, $CaLaNb_2TiO_{10}$, $La_2Ti_2NbO_{10}$, and $Ba_5Ta_4O_{15}$ ⬤ Strontium ⚪ Ruthenium ⬤ Oxygen Sr_2RuO_4 top view Sr_2RuO_4 side view	Intercalation with liquid crystals (*115*) Ion intercalation (protonation and ion exchange) (*116*) Amine surfactant (TBA$^+$) under sonication (*117*)	Ferroelectrics (*118*) Photochromic (*119*) Photoluminescent (*120*)	No (only by synthesis)

Oxides	Oxychalcogenides and oxypnictides: Oxychalcogenides, LaOCuCh (Ch, chalcogenide) and derivatives, $Sr_2MO_2Cu_{2-\delta}S_2$ (M = Mn, Co, Ni), $Sr_2MnO_2Cu_{2m-0.5}S_{m+1}$ (m = 1-3), $Sr_4Mn_3O_{7.5}Cu_2Ch_2$ (Ch=S, Se); oxypnictides, LaOFeAs ‖ ● Transition metal ● Pnictide ● Cation Ti_2Sb_2O top view Ti_2Sb_2O side view 	To our knowledge, these have never been exfoliated	Superconductivity (*121*) Magnetic properties (*121*) Catalyst (redox properties) (*121*) Batteries (*121*)	No (only by synthesis)
	Oxyhalides of transition metals, such as VOCl, CrOCl, FeOCl, NbO_2F, WO_2Cl_2, and $FeMoO_4Cl$ ● Transition metal ● Halide ● Oxygen FeOCl top view FeOCl side view 	Ion intercalation (*122*)	Batteries (*123*)	No (only by synthesis)

III–VI layered semiconductor	GaX (X = S, Se, Te); InX (X = S, Se Te)¶ ● S/Se/Te ● Ga/In GaSe top view GaSe side view 	Ion intercalation (*124*) Surfactant (*125*)	Nonlinear optical properties, poor thermal conductivity (*126*)	Some available (maybe purity issues), mostly synthesized
Layered α and γ zirconium phosphates and phosphonates	α-M^{IV} phosphates, α-$M^{IV}(O_3P–OH)_2$·H_2O; and α-Metal^{IV} phosphonates, $M^{IV}(O_3P–R)_2$· $n$$H_2O$# ● Oxygen ● Phosphorus ● Cation ● Water $CaHPO_4$ top view $CaHPO_4$ side view 	Intercalation (*127*) Exfoliation in water/acetone mixtures (*128*)	Drug delivery (*127*) Semiconductor for dye sensitized solar cells (*129*)	No (only by synthesis)

Clays (layered silicates)	2:1 Layered silicates**: Smectites, $M^{n+}_{x/n} \cdot yH_2O[Al_{4-x}Mg_x](Si_8)O_{20}(OH)_4$; talc, $[(Mg_3)(Si_2O_5)_2(OH)_2]$; vermiculite, $[Mg_6 \cdot Si_6Al_2/O_{20}(OH)_4][M^{n+}_{1/n}](Mg_6)$; biotite $[(MgFe)_3(Si_3Al)O_{10}(OH)_2]K$; phlogopite, $[(Mg_6)(Si_6Al_2)O_{20}(OH)_4]Ba$; fluorphlogopite, $[Mg_{11/4}(Si_6Al_2)O_{20}F_4][(M^{2+})_{3/2}]$; margarite, $[(Al_2)(Si_2Al_2)O_{10}(OH)_2]Ca$; and muscovite, $[(Al_2)(Si_3Al)O_{10}(OH)_2]K$	Dispersion in water (13) Intercalation (130) Polymer intercalation (131)	Catalysis (130) Composites (131) Lightweight nanocomposites for structural applications (132) Clay-dye complexes and photoactive materials (131) Organoclays as ionic and electronic conductors (composites with conductive polymers) (131) Thermal and barrier properties nanocomposites (133)	Natural minerals, available on the market

● Oxygen ● Cation
● Silicon ● Intercalates/-C/-OH

Vermiculite top view

Vermiculite side view

1:1 Layered Silicates ††: Kaolite, $[Al_4Si_4O_{10}](OH)_8$; halloysite, $Al_4Si_4O_{10}(OH)_8 \cdot 4H_2O$

● Aluminum ● Silicon
● Oxygen ● OH-

Kaolite top view

Kaolite side view

Layered double hydroxides (LDHs)	General formula: $M(II)_{1-x}M(III)_x(OH)_2(A^{n-})_{x/n} \cdot yH_2O$, where M(II) = divalent cation; M(III) = trivalent cation; A = interlayer anion; and $n-$ = charge on interlayer anion‡‡ ● Oxygen　● Cation　● Hydrogen Brucite $(Mg^{2+}_x, Mg^{3+}_x(OH)_2(A^{n-})_{x/n} \cdot yH_2O)$top view Brucite $(Mg^{2+}_x, Mg^{3+}_x(OH)_2(A^{n-})_{x/n} \cdot yH_2O)$ side view 	Intercalation (*134*) Surfactant-assisted exfoliation and intercalation of molecules (*135*) Surfactant exfoliation (*136*) Solvent exfoliation in DMF (*137*) Functionalization followed by exfoliation in solvents (*138*)	Biocompatible–bio-hybrids/drug delivery (*12, 134*) Bionanocomposites with functional and structural properties (*139*)	No, only by synthesis
Ternary transition metal carbides and nitrides	Derivatives from MAX phases, where M = transition metal; A = Al or Si; and X=C or N§§ ● Carbon　● Oxygen ● Titanium　● Hydrogen Ti3C2 	Extra oxygen and hydrogen at layers surface are present as a consequence of the exfoliation treatment with HF (*66, 67*).	Batteries and supercapacitors (*140*)	Yes

*These are iso-structural with TMDs.　†These are defect CdI2 structure types.　‡These are heavy metal halides (perovskite type) structurally similar to transition metal dihalides with organic ammonium interlayers.　§Protons emplaced between 2D of $Nb_3O_8^-$ anion nanosheets composed of NbO_6 octahedra.　‖They contain oxide layers separated by distinct layers, which contain the softer chalcogenide (S, Se, and Te) or pnictide (P, As, Sb, and Bi).　¶The building block has a trigonal structure, consisting of a pair of (M_3X_3) rings linked by M–M bonds. Layers interact through van der Waals forces between the X outermost planes.　#R is an organic radical, and n is the number of water molecules that can be intercalated in the interlayer region.　**The 2:1 notation means that the layers consist of two tetrahedral silicate sheets sandwiching one octahedral sheet.　††Layer consists of one tetrahedral silicate sheets and one octahedral sheet.　‡‡The structure of LDHs can be described by considering $Mg(OH)_2$, which consists of Mg^{2+} ions coordinated octahedrally by hydroxyl groups. The octahedral units share edges to form infinite, charge neutral layers. In an LDH, isomorphous replacement of a fraction of the Mg^{2+} ions with a trivalent cation, such as Al^{3+}, occurs and generates a positive charge on the layers that necessitates the presence of interlayer, charge-balancing, anions. The remaining free space of the interlayer is occupied by water of crystallization.　§§Layered M_2X, M_3X_2, M_4X_3, where M = transition metal and X = C or N, can be obtained after removal of the A layer with hydrofluoric acid (HF).
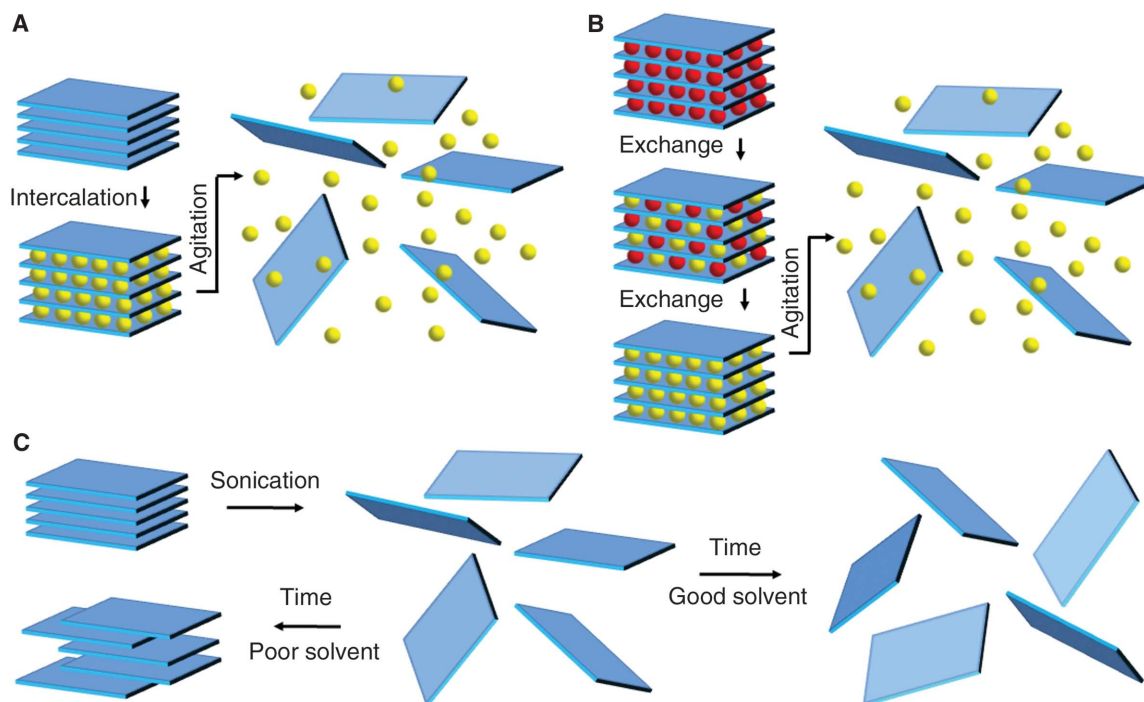
Fig. 2. Schematic description of the main liquid exfoliation mechanisms. (**A**) Ion intercalation. Ions (yellow spheres) are intercalated between the layers in a liquid environment, swelling the crystal and weakening the interlayer attraction. Then, agitation (such as shear, ultrasonication, or thermal) can completely separate the layers, resulting in an exfoliated dispersion. (**B**) Ion exchange. Some layered compounds contain ions between the layers so as to balance surface charge on the layers. These ions (red spheres) can be exchanged in a liquid environment for other, often larger ions (yellow spheres). As above, agitation results in an exfoliated dispersion. (**C**) Sonication-assisted exfoliation. The layered crystal is sonicated in a solvent, resulting in exfoliation and nanosheet formation. In "good" solvents—those with appropriate surface energy—the exfoliated nanosheets are stabilized against reaggregation. Otherwise, for "bad" solvents reaggregation and sedimentation will occur. This mechanism also describes the dispersion of graphene oxide in polar solvents, such as water. NB, solvent molecules are not shown in this figure.

contain an exchangeable interlayer of cationic counterions (8). For example, titanium dioxide (TiO_2) layered crystals tend to be negatively charged (because of the presence of both Ti^{3+} and Ti^{4+} ions) and so contain counter-ions such as Cs^+ between the layers to ensure charge neutrality (8, 25). Such ions can be exchanged for protons by soaking in acidic solutions. The protons can then be exchanged for bulky organic ions (for example, tetrabutylammonium cations), leading to substantial swelling. Alternatively, some clays containing small monovalent ions such as sodium swell from intercalation of water (13). In general, swelling facilitates exfoliation through ultrasonication or shear mixing to give negatively charged nanosheets (26).

A more recent strategy for exfoliation is to expose the layered material to ultrasonic waves in a solvent (27). Such waves generate cavitation bubbles that collapse into high-energy jets, breaking up the layered crystallites and producing exfoliated nanosheets. Modeling has shown that if the surface energy of the solvent is similar to that of the layered material, the energy difference between the exfoliated and reaggregated states will be very small, removing the driving force for reaggregation (28). Graphene, h-BN, TMDs, and some TMOs have been exfoliated in this way by using solvents such as N-methyl-pyrrolidone (28, 29). Similarly, ultrasonication in surfactant or polymer solutions gives nanosheets that are electrostatically or sterically stabilized (17, 30).

Pioneers

The exfoliation of layered compounds is an area of research that dates back several centuries. Modern research probably began with Webb and progressed via the work of chemists such as Schafhaeutl, Brodie, and Staudenmaier on the production of graphite intercalation compounds and graphite oxide in the mid-19th century (20). Although these early researchers knew of the laminar nature of graphite, the detailed structure was not known until the 1920s (28). Early attempts to understand exfoliated layered compounds used transmission electron microscopy (TEM) to image few- and possibly even mono-layer exfoliated graphene oxide as early as 1948. However, the limitations of available instrumentation made it impossible to verify whether monolayers were really observed (20, 31). The 1960s saw a flurry of activity on the cleavage (often using adhesive tape) of TMD crystals to produce nanosheets that approached monolayer thickness (32). This was complemented in 1967 by the demonstration that inorganic layered compounds—in this case, vermiculite clay—could be exfoliated in liquids by means of ion intercalation followed by shear mixing (26). In 1975, a similar technique was used to exfoliate TaS_2, possibly producing monolayers (33). Subsequently, the availability of cheap ultrasonic agitators provided a more effective energy source for exfoliation, leading to the demonstration of ion intercalation–assisted exfoliation of TaS_2, NbS_2, and MoS_2, as well as layered oxides (23, 34, 35). In these reports, TEM and x-ray diffraction suggested that monolayers had been produced. A decade later in 2000, the exfoliation of layered double hydroxides by means of ion exchange followed by stirring or reflux was demonstrated (36).

Much of this work has historically been limited by the instrumentation available. Early TEM characterization used techniques such as intensity analysis (34) or shadowing (32), which would not meet today's standards of proof for imaging a single layer. However, the development of scanning tunnelling microscopy (STM) and atomic force microscopy (AFM) in the 1980s and recent advances in scanning TEM have changed this entirely. By the time Geim *et al.* produced nanosheets through mechanical exfoliation (1), a new generation of scientific instrumentation with atomic-scale resolution had emerged in order to fully analyze exfoliated materials with unprecedented precision. The result has been a renewed surge in interest in these exotic, molecular-scale materials.

Recent Advances in Liquid Exfoliation

Although the exfoliation of layered materials has a long history, it was interest in graphene that
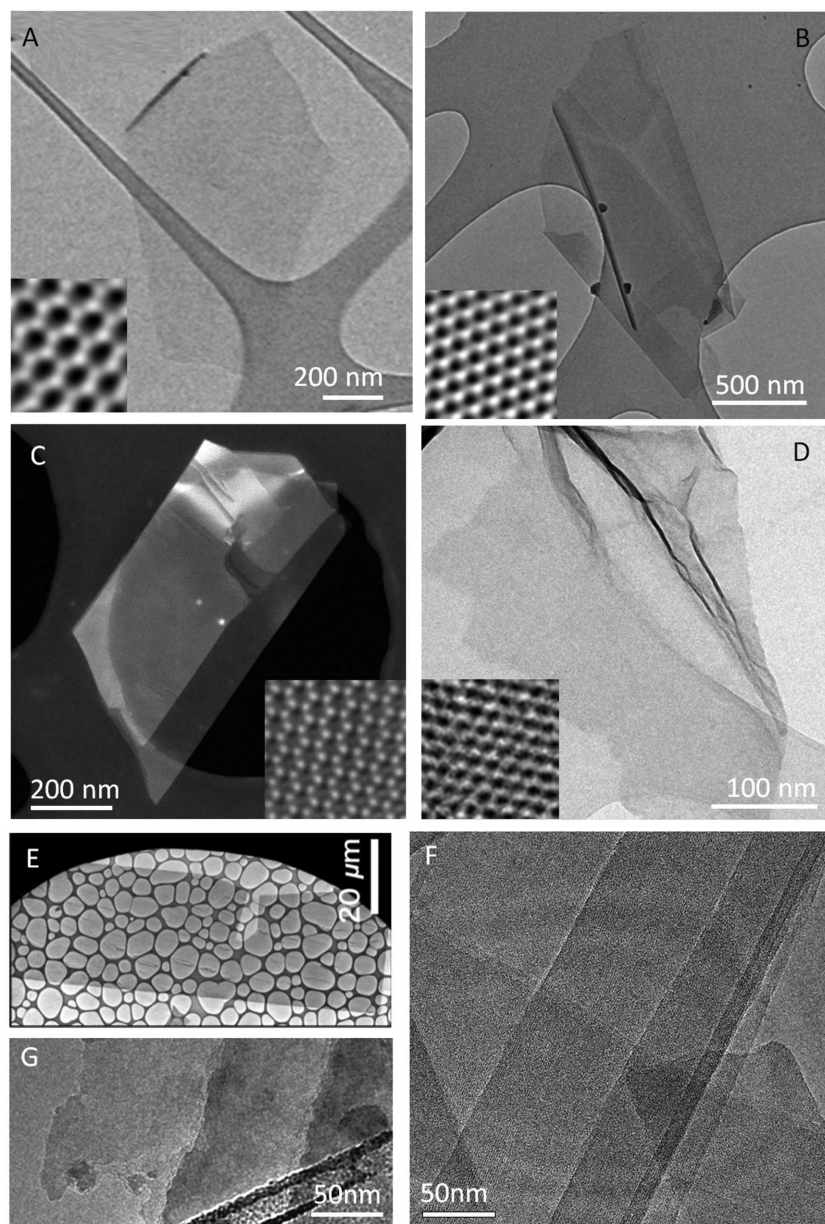
Fig. 3. TEM images of liquid exfoliated nanosheets. (**A**) A graphene nanosheet exfoliated by means of sonication in the solvent *N*-methyl-pyrrolidone (*27*). (**B**) A h-BN nanosheet exfoliated by means of sonication in the solvent isopropanol (*29*). (**C**) An MoS$_2$ nanosheet exfoliated by means of sonication in an aqueous surfactant solution (*58*). (**D**) An MoS$_2$ nanosheet exfoliated by means of Li ion intercalation (*22*). (**E**) A TiO$_2$ nanosheet exfoliated by means of ion exchange (*25*). (**F**) Functionalized layered double hydroxide nanosheets exfoliated by means of sonication in ethanol (*65*). (**G**) Hydroxylated metal carbide nanosheets exfoliated by means of sonication in methanol (*66*). Where available, high-resolution images have been included as insets. All images were adapted from the sources as referenced.

addition to the previously undiscovered electronic properties described above, monolayer graphene displays the highest strength and the highest thermal conductivity ever recorded (*1–3*). Very soon, it became clear that such a material would be required in much larger quantities than mechanical cleavage could deliver. It was immediately obvious that such scalable production might be achieved through liquid exfoliation (*40*).

One of the first approaches to liquid exfoliation was the oxidization of graphite. In 2006, Ruoff *et al*. demonstrated platelets of graphite oxide with monolayer thickness (*20*). Now known as graphene oxide (GO), this material is electrically insulating, although it can be rendered conducting via reduction (*20*). The oxidation allows one to control the amount and type of attached oxides, potentially enabling control of electrical conductivity and luminescence (*41*). A disadvantage of this method is that it necessarily introduces chemical groups and defects that scatter electrons, giving relatively high resistivity. Graphene oxide exfoliation has been the subject of many papers and reviews (*20*).

Around the time of Geim's seminal paper, McEwan *et al*. produced good-quality nanographite by sonicating graphite in the solvent dichlorobenzene (*42*). However, monolayer graphene was not observed in this work. It was not until 4 years later that liquid-exfoliated monolayer graphene was produced by ultrasonicating graphite in solvents such as *N*-methyl pyrrolidone and di-methyl formamide (*27*, *43*). It was found that exfoliation was only achieved by using solvents with surface tension close to 40 mJ/m^2. Theoretical modeling showed that for such solvents, the solvent-graphene interaction is optimized so that the energetic cost of exfoliation was minimized (*27*, *44*, *45*). This method resulted in low-concentration dispersions of small but high-quality, defect-free graphene flakes. Recent improvements have substantially enhanced both the dispersed concentration (up to 30 mg/ml), the nanosheet size (up to 5 μm), and the range of solvents (*28*, *45–48*). This method is promising for applications in which good electrical performance is required. For example, solvent-exfoliated graphene has been used to prepare transparent electrodes for liquid crystal devices (*43*). Recent results on printed electronic circuits have yielded mobility values of ~100 cm^2/Vs (*49*), which are some of the highest for any chemically exfoliated graphenes. In addition, liquid exfoliation of graphene with minimal lattice defects allows the effective reinforcement of polymers (*17*).

Unfortunately, the most useful solvent of all, water, has a surface tension of 72 mJ/m^2 and so cannot by itself exfoliate graphene. However, if graphite is ultrasonicated in aqueous surfactant solutions, graphene can be exfoliated and stabilized against reaggregation through electrostatic effects (*30*, *50–53*). Similarly, when ultrasonicated in polymer solutions, by using both water and organic solvents, graphene can be exfoliated and stabilized through steric effects

stimulated renewed curiosity in this area. For this reason, we outline the recent developments in the liquid exfoliation of layered crystals, using Geim and Novoselov's 2004 paper describing the properties of exfoliated graphene as a starting point.

In a series of papers beginning in 2004 (*1*, *3*, *37*, *38*), Geim, Novoselov, and collaborators showed that monolayers of graphene and other 2D materials could be removed from their parent crystals by means of mechanical exfoliation and placed on substrates of choice. This was some-

what surprising because theoretical studies had suggested that 2D materials should be intrinsically unstable after exfoliation (*2*). This apparent contradiction was later resolved with the suggestion that the exfoliated monolayers are stabilized by the formation of ripples that effectively extend the 2D material into the third dimension (*39*). However, the most exciting result of exfoliation was the demonstration that graphene displayed electronic, mechanical, and thermal properties not seen in any other material. For example, in

(*17*, *54*, *55*). The latter method is particularly useful as a method for producing polymer-nanosheet composites (*17*).

Similar methods have recently been used to exfoliate both h-BN (*4*, *29*, *56*, *57*) and a range of TMDs in both solvents and surfactant or polymer solutions (*29*, *54*, *58*–*61*). Dispersions of TMDs such as MoS_2, WS_2, $MoSe_2$, $MoTe_2$, $TaSe_2$, and $NbSe_2$ (*58*) were obtained at concentrations as high as 40 mg/ml (*61*). As with graphene, dispersion works for solvents or solvent blends (*62*) with surface energies that minimize the energetic cost of exfoliation (*29*). TMDs prepared with this scalable method have attracted interest as composite fillers (*63*) and for energy storage (*64*). For example, Smith *et al.* have demonstrated solution-processed MoS_2/nanotube composite cathodes for Li ion batteries with reversible capacities of >200 mA h g^{-1} (*58*). Chemical pretreatment also facilitates exfoliation by means of sonication in solvents. For example, functionalization allows the exfoliation of LDHs in alcohols (*65*). Similarly, acid treatment of metal aluminum carbides/nitrides produces the MXenes—metal carbide nanosheets with fluorinated or hydroxylated surfaces—that can be exfoliated in methanol (*66*, *67*).

A number of advances have been made in the exfoliation of layered materials via ion intercalation. Strano *et al.* have demonstrated that dispersions of predominately bi- and tri-layer graphene can be produced from graphite intercalation compounds by thermal expansion followed by sonication in surfactant solution (*21*). Eda *et al.* have used ion intercalation to exfoliate MoS_2 (*22*), obtaining photoluminescent monolayers. Recently, Zeng *et al.* demonstrated electrochemical Li insertion followed by exfoliation for MoS_2, WS_2, TiS_2, TaS_2, ZrS_2, and graphite (*68*). The resultant nanosheets were fabricated into transistors and sensors. Recently, Xiao *et al.* (*63*) reported using exfoliated MoS_2 to prepare MoS_2/polyethylene oxide nanocomposites as battery electrodes with greatly improved lithiation capacity and cycling behavior. Du *et al.* (*69*) prepared MoS_2 anode electrodes by means of an exfoliation and restacking process, improving stability and achieving capacities as high as 800 mA h g^{-1}. Additionally, exfoliation by means of ion intercalation has been demonstrated for V-VI layered compounds such as Bi_2Te_3 and Bi_2Se_3 (*70*).

Of particular interest are layered metal oxides owing to their interesting electronic and dielectric properties (*9*, *10*). Because of these properties, their exfoliation has been studied since at least 1990 (*35*) and mainly involves ion exchange followed by agitation (*9*). Exfoliated oxide nanosheets are most often wide-bandgap semiconductors, making them promising for applications such as photocatalysts or high-dielectric constant materials (*8*, *10*). Alternatively, exfoliated MnO_2 and RuO_2 nanosheets are either redox-active or semi-metallic (*8*, *10*) and have demonstrated high performance as electrochemical supercapacitors and battery materials (*8*, *10*). Furthermore, the availa-

bility of 2D semiconducting nanosheets opens up possibilities for designing more complex nanodevices, such as photoconducting cells, p-n junctions, and field-effect transistors (FETs) (*8*, *9*). Colloidal dispersions of exfoliated $Cs_4W_{11}O_{36}^{2-}$ nanosheets are photochromic and superior to commonly used materials such as WO_3 (*8*). MnO_2 has also been exfoliated by means of ultrasonication in aqueous surfactant solutions (*58*), suggesting that this facile route can be applied to other layered oxides.

Intercalated layered double hydroxides were first successfully delaminated by Adachi-Pagano *et al.* by exchanging the interlayer anions with dodecyl-sulfate under reflux in butanol (*71*). Recent studies have focused on exfoliating such ion-exchanged materials in solvents such as fomamide (*71*) and water (*72*). High-concentration (~40 g/L) dispersions of mono- and few-layer LDHs were reported by Wu *et al.* (*73*). Liquid exfoliated LDHs have found applications in areas as diverse as drug delivery and water treatment (*8*).

Although liquid exfoliation of clay minerals such as montmorillonite or vermiculites is reasonably well known, recent work has focused on dispersing clay nanosheets in hydrophobic polymers for composite applications. This has been achieved by exchanging the charge-balancing ions with organocations so as to form organoclays (*74*).

It has recently been shown that other layered chalcogenides such as metal phosphorous trichalcogenides ($CdPS_3$ and $MnPS_3$, for example) can also be exfoliated into single layers by means of ion exchange (*75*). Details of exfoliation strategies for a wide range of layered materials are given in Table 1.

Potential Applications of Liquid-Exfoliated Nanosheets

Liquid exfoliation represents a versatile, scalable, and sustainable route for production of 2D nanosheets. In addition, access to suspensions of nanosheets permits processing in ways that would otherwise be difficult or impossible. For example, processing from liquids allows the deposition of individual nanosheets on surfaces and the formation of thin or free-standing films; facilitates mixing with other nanomaterials to form heterostructured solids; and enables insertion, as fillers, into polymer matrices (Fig. 4).

The ability to invoke different phases of 2D materials via tuning the exfoliation chemistry opens up an exciting range of possibilities. For example, exfoliation via electrochemical ion intercalation leads to realization of the metallic (1T) phase in layered transition metal chalcogenides, which cannot be accessed through other synthesis techniques (*76*). Some applications include electrodes for energy-storage devices, high-performance fillers for polymer-based composites, electro- and photocatalysis for hydrogen evolution, nano- and large-area electronics and opto-electronics, and low-friction additives in lubrication systems.

The production of inexpensive 2D nanosheets holds promise for multifunctional polymer com-

posites. Polymer-clay composites can display improved mechanical and barrier properties, usually at loading levels from a few percent to a few tens of percent (*77*). Because of the potentially high aspect ratio of exfoliated graphene, polymers loaded with graphene display reinforcement (*17*), conductivity enhancement (*78*), and barrier properties (*79*) at loading fractions below 1 volume %. Solvent processing of 2D nanosheets makes composite fabrication straightforward and will extend the suite of 2D fillers beyond clays and graphene (*4*, *29*, *80*). Liquid exfoliation also allows the formation of unusual composites consisting of mixtures of nanosheets, nanotubes, and other nanostructures (Fig. 4) (*29*, *58*). This results in synergetic effects; for example, composites of WS_2 and carbon nanotubes display very high conductivity but retain much of the character of WS_2 films (*29*, *58*, *81*). Such composites are promising for applications in photovoltaic or thermoelectric devices and as electrodes for supercapacitors or batteries.

Supercapacitor electrodes formed from chemically exfoliated graphene nanosheets have yielded energy densities of 20 W h kg^{-1} for packaged devices, approaching those of lead-acid batteries (*82*). Recent results on restacked nanosheet films indicate that they maintain their structural integrity upon intercalation and deintercalation (*58*). The wide range of 2D materials available with varying electrochemical properties makes them ideal for energy storage. Initial measurements indicate that their capacitive capability is very high, although issues relating to substantial loss after the first few cycles remain. Choosing the correct combinations of materials will allow multiple properties (such as surface area, conductivity, and electrochemical stability) to be simultaneously improved so as to provide flexibility for designing electrodes for batteries and supercapacitors. For example, materials such as VS_2, MoO_3, and MnO_2 could be useful for efficient energy storage.

The possibility that layered materials could catalyze the production of hydrogen from water, for use as a fuel, is a critically important application. The edge molybdenum sites on TMDs are highly active for hydrogen evolution reactions and thus are being considered as electrodes for water-splitting by using sunlight. With ion-exfoliated 2D TMDs, the presence of a metallic (1T) phase makes the entire basal plane catalytically active, leading to an improvement in the catalytic activity and a substantial increase in the number of active catalytic sites (*83*). Oxide nanosheets (such as TiO_2 and MoO_3) are also candidates for hydrogen evolution catalysts (*84*).

Liquid-phase exfoliation facilitates the integration of the materials into large-area electronics through the well-known solution-based techniques such as inkjet printing (*49*) and roll-to-roll coating. Recent results have indicated that the electronic structure of the 2D nanosheets is largely preserved after liquid exfoliation so that fundamental processes can be observed in individual
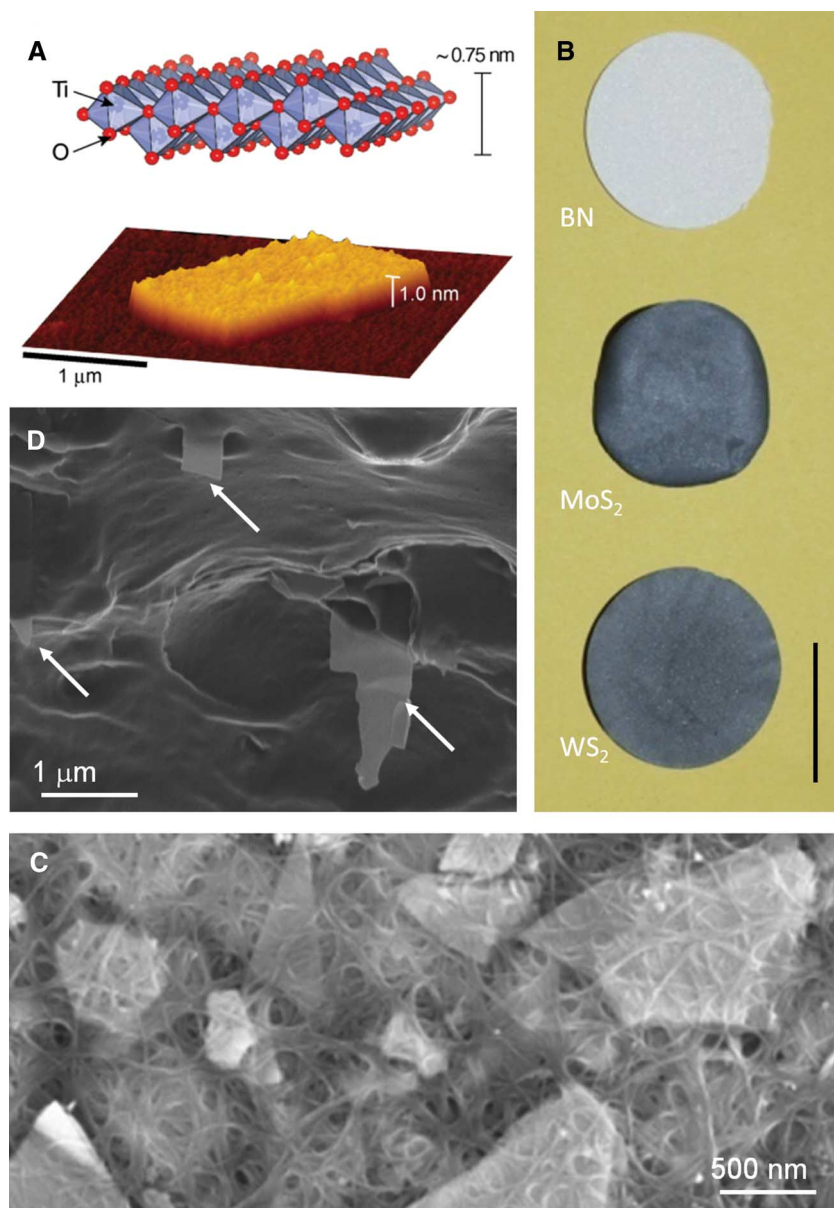
Fig. 4. Once layered materials have been exfoliated in liquids, they can be easily processed into a range of structures. (**A**) TiO$_2$ nanosheets deposited onto a substrate and imaged by means of AFM (*10*). (**B**) Solution-processed, free-standing films of randomly arranged nanosheets of h-BN, MoS$_2$, and WS$_2$ (*29*). Scale bar, 25 mm. (**C**) A composite film of WS$_2$ nanosheets in a matrix of randomly arranged carbon nanotubes (*29*). (**D**) Solvent-exfoliated graphene nanosheets (arrows) embedded in a polymer matrix (*17*). All images were adapted from the sources as referenced.

sheets. For example, because exfoliated oxides retain their excellent dielectric properties, they can be used as high-κ dielectrics in nanoelectronics (*10*). Alternatively, stacking of different layered perovskites allows the fabrication of artificial multi-ferroic materials for use in future oxide-based electronics and memory devices. Exfoliated oxide nanosheets may also be used in more complex nanodevices, such as photoconducting cells, p-n junctions, and field-effect transistors (*8, 10*). Alternatively, MoS$_2$ shows exceptionally stable transistor operation under very large mechanical deformation (*85*). The relatively undisturbed electronic structure coupled with flexibility makes MoS$_2$ and other 2D materials useful for next-generation large-area electronics and opto-electronics on plastic and paper platforms. In particular, large-area, solution-cast, TMD thin-film transistors with mobility of ~10 to 50 cm^2/V s could replace doped oxide semiconductors for back-plane switching in flexible and transparent displays.

More exotic applications of layered 2D materials will arise from the stacking and seamless integration of specific combinations of materials in order to access fundamental properties such as superconductivity and condensates (*86*). The integration could be in the vertical or lateral direction so as to allow for different device concepts. The ability to access metallic and semiconducting phases in 2D materials with electrochemical exfoliation also provides opportunities for designing molecular-scale heterostructures with atomically coherent junctions (*24*). These types of super-lattice structures could be easily synthesized from liquid dispersions.

Outlook

Our ability to employ straightforward techniques to exfoliate materials points to a productive future in this area. However, a number of substantial challenges remain. Although ultrasonication-assisted solvent exfoliation displays great promise, it also has a number of limitations in its current form. For example, the monolayer yield is generally no more than a few tens of percent by number, which is far too low for many applications. As such, it will be necessary to develop methods to monitor and increase both the monomer yield and indeed the lateral flake size. For ion intercalation–based methods, the time required to achieve exfoliation must be reduced. Crucially, the scale-up of liquid exfoliation must be demonstrated. The ultimate aim must be production on an industrial scale (more than kilograms per day)—a goal that seems relatively far off for defect-free materials. This will almost certainly require exfoliation methods that do not rely on ultrasonication, a method that has limited scalability. However, an achievable early target would be a production rate of grams of exfoliated nanosheets per hour.

It will be important to demonstrate exfoliation of a wider range of layered materials. To date, liquid exfoliation has produced graphene, h-BN, a number of TMDs, a range of clays, many oxides and hydroxides, and a scattering of other exfoliated nanosheets. However, there is a galaxy of other materials (Table 1) offering a rich set of distinct features that have not yet been exfoliated but should be amenable to the methods described above. For example, because layered GaSe and InSe are photoluminescent, liquid exfoliation could lead to next-generation solution-processed, photostable light-emitting diodes. Alternatively, V-VI layered compounds (such as Bi$_2$Te$_3$ and Bi$_2$Se$_3$) could form the basis of solution-processed thermoelectric materials (*29, 58*).

In addition, exfoliation in liquids will be a good starting point for subsequent chemical modification of nanosheets. For example, chemical functionalization will allow controlled modification of the properties of exfoliated nanosheets for applications in composites, targeted drug delivery, or sensing. It will be critical to develop the chemistry required to attach a wide range of chemical groups to both nanosheet basal plane and edge in a controlled way.

Last, there are a number of cases in which 2D materials might be produced from starting materials that differ considerably from the layered crystals described above. Specifically, we consider materials that lack a clearly defined van der

Waals gap. There are entire families of materials that are made of extended layers carrying negative or positive charges and are separated by charge-balancing cations or anions, respectively. Such systems will have just as interesting chemical and physical properties as the neutral layered analogs. Some examples include the semiconducting $NaInSe_2$, $K_2Cd_3S_4$, $K_2Fe_4Se_5$, the metallic KCu_4S_3, $BaFe_2As_2$, and the superconducting KFe_2As_2. Instead of weak van der Waals forces, much stronger electrostatic interactions hold these layers together. In these cases, separation of the layers will require the apportioning of the charge-balancing ions between them to partition evenly on both layers coming apart. This will create surfaces that need to be neutral. Therefore, innovative chemical methods that can dismantle the solid-state lattices and stabilize such surfaces will be required. That such approaches are feasible is evidenced by the chemical modification and subsequent exfoliation of Ti_3AlC_2—a material without a van der Waals gap—to give nanosheets of $Ti_3C_2F_2$ and $Ti_3C_2(OH)_2$ (*67*).

As exfoliation methods increase in their sophistication and effectiveness, layered materials will yield a host of new 2D systems to explore. The diverse range of properties of known layered crystals means that their exfoliated counterparts will be equally diverse, leading to applications in electronics, photonics, energy storage, structural composites, drug delivery, barrier layers, and coatings, to name but a few. We envisage exfoliated nanosheets becoming central to nanotechnology in the 21st century.

References and Notes

1. A. K. Geim, Graphene: Status and prospects. *Science* **324**, 1530 (2009). doi: 10.1126/science.1158877; pmid: 19541989
2. A. K. Geim, K. S. Novoselov, The rise of graphene. *Nat. Mater.* **6**, 183 (2007). doi: 10.1038/nmat1849; pmid: 17330084
3. K. S. Novoselov *et al.*, A roadmap for graphene. *Nature* **490**, 192 (2012). doi: 10.1038/nature11458; pmid: 23060189
4. D. Golberg *et al.*, Boron nitride nanotubes and nanosheets. *ACS Nano* **4**, 2979 (2010). doi: 10.1021/nn1006495; pmid: 20462272
5. Q. H. Wang, K. Kalantar-Zadeh, A. Kis, J. N. Coleman, M. S. Strano, Electronics and optoelectronics of two-dimensional transition metal dichalcogenides. *Nat. Nanotechnol.* **7**, 699 (2012). doi: 10.1038/nnano.2012.193; pmid: 23132225
6. J. A. Wilson, A. D. Yoffe, The transition metal dichalcogenides discussion and interpretation of the observed optical, electrical and structural properties. *Adv. Phys.* **18**, 193 (1969). doi: 10.1080/00018736900101307
7. C. C. Coleman, H. Goldwhite, W. Tikkanen, A review of intercalation in heavy metal iodides. *Chem. Mater.* **10**, 2794 (1998). doi: 10.1021/cm980211r
8. R. Z. Ma, T. Sasaki, Nanosheets of oxides and hydroxides: Ultimate 2D charge-bearing functional crystallites. *Adv. Mater.* **22**, 5082 (2010). doi: 10.1002/adma.201001722; pmid: 20925100
9. M. Osada, T. Sasaki, Exfoliated oxide nanosheets: New solution to nanoelectronics. *J. Mater. Chem.* **19**, 2503 (2009). doi: 10.1039/b820160a
10. M. Osada, T. Sasaki, Two-dimensional dielectric nanosheets: Novel nanoelectronics from nanocrystal building blocks. *Adv. Mater.* **24**, 210 (2012). doi: 10.1002/adma.201103241; pmid: 21997712
11. M. A. Bizeto, A. L. Shiguihara, V. R. L. Constantino, Layered niobate nanosheets: Building blocks for advanced materials assembly. *J. Mater. Chem.* **19**, 2512 (2009). doi: 10.1039/b821435b
12. P. Nalawade, B. Aware, V. J. Kadam, R. S. Hirlekar, *J. Sci. Ind. Res. (India)* **68**, 267 (2009).
13. P. F. Luckham, S. Rossi, The colloidal and rheological properties of bentonite suspensions. *Adv. Colloid Interface Sci.* **82**, 43 (1999). doi: 10.1016/S0001-8686(99)00005-6
14. B. Velde, *Introduction to Clay minerals: Chemistry, Origins, Uses, and Environmental Significance* (Chapman & Hall, London, UK, 1992).
15. V. Grasso, Ed., *Electronic Structure and Electronic Transitions in Layered Materials* (Springer, New York, 1986).
16. M. Z. Hasan, C. L. Kane, Colloquium: Topological insulators. *Rev. Mod. Phys.* **82**, 3045 (2010). doi: 10.1103/RevModPhys.82.3045
17. P. May, U. Khan, A. O'Neill, J. N. Coleman, Approaching the theoretical limit for reinforcing polymers with graphene. *J. Mater. Chem.* **22**, 1278 (2012). doi: 10.1039/c1jm15467b
18. K. F. Mak, C. Lee, J. Hone, J. Shan, T. F. Heinz, Atomically thin MoS_2: A new direct-gap semiconductor. *Phys. Rev. Lett.* **105**, 136805 (2010). doi: 10.1103/PhysRevLett.105.136805; pmid: 21230799
19. A. Splendiani *et al.*, Emerging photoluminescence in monolayer MoS_2. *Nano Lett.* **10**, 1271 (2010). doi: 10.1021/nl903868w; pmid: 20229981
20. D. R. Dreyer, S. Park, C. W. Bielawski, R. S. Ruoff, The chemistry of graphene oxide. *Chem. Soc. Rev.* **39**, 228 (2010). doi: 10.1039/b917103g; pmid: 20023850
21. C. J. Shih *et al.*, Bi- and trilayer graphene solutions. *Nat. Nanotechnol.* **6**, 439 (2011). doi: 10.1038/nnano.2011.94; pmid: 21706026
22. G. Eda *et al.*, Photoluminescence from chemically exfoliated MoS_2. *Nano Lett.* **11**, 5111 (2011). doi: 10.1021/nl201874w; pmid: 22035145
23. P. Joensen, R. F. Frindt, S. R. Morrison, Single-layer MoS_2. *Mater. Res. Bull.* **21**, 457 (1986). doi: 10.1016/0025-5408(86)90011-5
24. G. Eda *et al.*, Coherent atomic and electronic heterostructures of single-layer MoS_2. *ACS Nano* **6**, 7311 (2012). doi: 10.1021/nn302422x; pmid: 22799455
25. T. Tanaka, Y. Ebina, K. Takada, K. Kurashima, T. Sasaki, Oversized titania nanosheet crystallites derived from flux-grown layered titanate single crystals. *Chem. Mater.* **15**, 3564 (2003). doi: 10.1021/cm034307j
26. G. F. Walker, W. G. Garrett, Chemical exfoliation of vermiculite and the production of colloidal dispersions. *Science* **156**, 385 (1967). doi: 10.1126/science.156.3773.385; pmid: 17812385
27. Y. Hernandez *et al.*, High-yield production of graphene by liquid-phase exfoliation of graphite. *Nat. Nanotechnol.* **3**, 563 (2008). doi: 10.1038/nnano.2008.215; pmid: 18772919
28. J. N. Coleman, Liquid exfoliation of defect-free graphene. *Acc. Chem. Res.* **46**, 14 (2013). doi: 10.1021/ar300009f; pmid: 22433117
29. J. N. Coleman *et al.*, Two-dimensional nanosheets produced by liquid exfoliation of layered materials. *Science* **331**, 568 (2011). doi: 10.1126/science.1194975; pmid: 21292974
30. M. Lotya *et al.*, Liquid phase production of graphene by exfoliation of graphite in surfactant/water solutions. *J. Am. Chem. Soc.* **131**, 3611 (2009). doi: 10.1021/ja807449u; pmid: 19227978
31. G. Ruess, F. Vogt, Höchstlamellarer Kohlenstoff aus Graphitoxyhydroxyd. *Mon. Chem.* **78**, 222 (1948). doi: 10.1007/BF01141527
32. R. F. Frindt, Single crystals of MoS_2 several molecular layers thick. *J. Appl. Phys.* **37**, 1928 (1966). doi: 10.1063/1.1708627
33. D. W. Murphy, G. W. Hull, Monodispersed tantalum disulfide and adsorption complexes with cations. *J. Chem. Phys.* **62**, 973 (1975). doi: 10.1063/1.430513
34. C. Liu, O. Singh, P. Joensen, A. E. Curzon, R. F. Frindt, X-ray and electron microscopy studies of single-layer TaS_2 and NbS_2. *Thin Solid Films* **113**, 165 (1984). doi: 10.1016/0040-6090(84)90025-7
35. M. M. J. Treacy, S. B. Rice, A. J. Jacobson, J. T. Lewandowski, Electron microscopy study of delamination in dispersions of the perovskite-related layered phases $K[Ca_2Na_{n-3}NbnO_{3n-1}]$: Evidence for single-layer formation. *Chem. Mater.* **2**, 279 (1990). doi: 10.1021/cm00009a018
36. M. Adachi-Pagano, C. Forano, J. P. Besse, Delamination of layered double hydroxides by use of surfactants. *Chem. Commun. (Camb.)* **1**, 91 (2000). doi: 10.1039/a908251d
37. K. S. Novoselov *et al.*, Electric field effect in atomically thin carbon films. *Science* **306**, 666 (2004). doi: 10.1126/science.1102896; pmid: 15499015
38. K. S. Novoselov *et al.*, Two-dimensional atomic crystals. *Proc. Natl. Acad. Sci. U.S.A.* **102**, 10451 (2005). doi: 10.1073/pnas.0502848102; pmid: 16027370
39. J. C. Meyer *et al.*, The structure of suspended graphene sheets. *Nature* **446**, 60 (2007). doi: 10.1038/nature05545; pmid: 17330039
40. R. Ruoff, Graphene: Calling all chemists. *Nat. Nanotechnol.* **3**, 10 (2008). doi: 10.1038/nnano.2007.432; pmid: 18654440
41. G. Eda, M. Chhowalla, Chemically derived graphene oxide: Towards large-area thin-film electronics and optoelectronics. *Adv. Mater.* **22**, 2392 (2010). doi: 10.1002/adma.200903689; pmid: 20432408
42. J. S. Bunch, Y. Yaish, M. Brink, K. Bolotin, P. L. McEuen, Coulomb oscillations and Hall effect in quasi-2D graphite quantum dots. *Nano Lett.* **5**, 287 (2005). doi: 10.1021/nl048111+; pmid: 15794612
43. P. Blake *et al.*, Graphene-based liquid crystal device. *Nano Lett.* **8**, 1704 (2008). doi: 10.1021/nl080649i; pmid: 18444691
44. J. M. Hughes, D. Aherne, J. N. Coleman, Generalizing solubility parameter theory to apply to one- and two-dimensional solutes and to incorporate dipolar interactions. *J. Appl. Polym. Sci.* **127**, 4483 (2013). doi: 10.1002/app.38051
45. Y. Hernandez, M. Lotya, D. Rickard, S. D. Bergin, J. N. Coleman, Measurement of multicomponent solubility parameters for graphene facilitates solvent discovery. *Langmuir* **26**, 3208 (2010). doi: 10.1021/la903188a; pmid: 19883090
46. A. O'Neill, U. Khan, P. N. Nirmalraj, J. Boland, J. N. Coleman, Graphene dispersion and exfoliation in low boiling point solvents. *J. Phys. Chem. C* **115**, 5422 (2011). doi: 10.1021/jp110942e
47. A. B. Bourlinos, V. Georgakilas, R. Zboril, T. A. Steriotis, A. K. Stubos, Liquid-phase exfoliation of graphite towards solubilized graphenes. *Small* **5**, 1841 (2009). doi: 10.1002/smll.200900242; pmid: 19408256
48. U. Khan, A. O'Neill, M. Lotya, S. De, J. N. Coleman, High-concentration solvent exfoliation of graphene. *Small* **6**, 864 (2010). doi: 10.1002/smll.200902066; pmid: 20209652
49. F. Torrisi *et al.*, Inkjet-printed graphene electronics. *ACS Nano* **6**, 2992 (2012). doi: 10.1021/nn2044609; pmid: 22449258
50. M. Lotya, P. J. King, U. Khan, S. De, J. N. Coleman, High-concentration, surfactant-stabilized graphene dispersions. *ACS Nano* **4**, 3155 (2010). doi: 10.1021/nn1005304; pmid: 20455583
51. R. J. Smith, M. Lotya, J. N. Coleman, The importance of repulsive potential barriers for the dispersion of graphene using surfactants. *New J. Phys.* **12**, 125008 (2010). doi: 10.1088/1367-2630/12/12/125008
52. S. Vadukumpully, J. Paul, S. Valiyaveettil, Cationic surfactant mediated exfoliation of graphite into graphene flakes. *Carbon* **47**, 3288 (2009). doi: 10.1016/j.carbon.2009.07.049
53. A. A. Green, M. C. Hersam, *Nano Lett.* **9**, 4031 (2009).
54. P. May, U. Khan, J. M. Hughes, J. N. Coleman, Role of solubility parameters in understanding the steric stabilization of exfoliated two-dimensional nanosheets by adsorbed polymers. *J. Phys. Chem. C* **116**, 11393 (2012). doi: 10.1021/jp302365w
55. A. B. Bourlinos *et al.*, Aqueous-phase exfoliation of graphite in the presence of polyvinylpyrrolidone for the production of water-soluble graphenes. *Solid State Commun.* **149**, 2172 (2009). doi: 10.1016/j.ssc.2009.09.018

56. Y. Lin, T. V. Williams, J. W. Connell, Soluble, Exfoliated hexagonal boron nitride nanosheets. *Journal of Physical Chemistry Letters* **1**, 277 (2010). doi: 10.1021/jz9002108

57. C. Y. Zhi, Y. Bando, C. C. Tang, H. Kuwahara, D. Golberg, Large-scale fabrication of boron nitride nanosheets and their utilization in polymeric composites with improved thermal and mechanical properties. *Adv. Mater.* **21**, 2889 (2009). doi: 10.1002/adma.200900323

58. R. J. Smith et al., Large-scale exfoliation of inorganic layered compounds in aqueous surfactant solutions. *Adv. Mater.* **23**, 3944 (2011). doi: 10.1002/adma.201102584; pmid: 21796689

59. G. Cunningham et al., Solvent exfoliation of transition metal dichalcogenides: Dispersibility of exfoliated nanosheets varies only weakly between compounds. *ACS Nano* **6**, 3468 (2012). doi: 10.1021/nn300503e; pmid: 22394330

60. Y. G. Yao et al., Large-scale production of two-dimensional nanosheets. *J. Mater. Chem.* **22**, 13494 (2012). doi: 10.1039/c2jm30587a

61. A. O'Neill, U. Khan, J. N. Coleman, Preparation of high concentration dispersions of exfoliated MoS_2 with increased flake size. *Chem. Mater.* **24**, 2414 (2012). doi: 10.1021/cm301515z

62. K. G. Zhou, N. N. Mao, H. X. Wang, Y. Peng, H. L. Zhang, A mixed-solvent strategy for efficient exfoliation of inorganic graphene analogues. *Angew. Chem. Int. Ed.* **50**, 10839 (2011). doi: 10.1002/anie.201105364

63. J. Xiao et al., Exfoliated MoS_2 nanocomposite as an anode material for lithium ion battery. *Chem. Mater.* **22**, 4522 (2010). doi: 10.1021/cm101254j

64. Y. L. Liang et al., Rechargeable Mg batteries with graphene-like MoS_2 cathode and ultrasmall Mg nanoparticle anode. *Adv. Mater.* **23**, 640 (2011). doi: 10.1002/adma.201003560; pmid: 21274912

65. Y. Xu, K. Kominami, Y. Ishikawa, Q. Feng, Layered hydroxide nickel benzoates: Hydrothermal synthesis, structure characterization, and exfoliation reaction. *J. Colloid Interface Sci.* **386**, 107 (2012). doi: 10.1016/j.jcis.2012.07.046; pmid: 22897953

66. M. Naguib et al., Two-dimensional transition metal carbides. *ACS Nano* **6**, 1322 (2012). doi: 10.1021/nn204153h; pmid: 22279971

67. M. Naguib et al., Two-dimensional nanocrystals produced by exfoliation of Ti_3 AlC2. *Adv. Mater.* **23**, 4248 (2011). doi: 10.1002/adma.201102306; pmid: 21861270

68. Z. Y. Zeng et al., Single-layer semiconducting nanosheets: High-yield preparation and device fabrication. *Angew. Chem. Int. Ed.* **50**, 11093 (2011). doi: 10.1002/anie.201106004

69. G. D. Du et al., Superior stability and high capacity of restacked molybdenum disulfide as anode material for lithium ion batteries. *Chem. Commun. (Camb.)* **46**, 1106 (2010). doi: 10.1039/b920277c; pmid: 20126728

70. Z. F. Ding et al., Lithium intercalation and exfoliation of layered bismuth selenide and bismuth telluride. *J. Mater. Chem.* **19**, 2588 (2009). doi: 10.1039/b820226e

71. R. Z. Ma, Z. P. Liu, L. Li, N. Iyi, T. Sasaki, Exfoliating layered double hydroxides in formamide: A method to obtain positively charged nanosheets. *J. Mater. Chem.* **16**, 3809 (2006). doi: 10.1039/b605422f

72. T. Hibino, M. Kobayashi, Delamination of layered double hydroxides in water. *J. Mater. Chem.* **15**, 653 (2005). doi: 10.1039/b416913a

73. Q. L. Wu, A. Olafsen, O. B. Vistad, J. Roots, P. Norby, Delamination and restacking of a layered double hydroxide with nitrate as counter anion. *J. Mater. Chem.* **15**, 4695 (2005). doi: 10.1039/b511184f

74. S. S. Ray, M. Okamoto, *Prog. Polym. Sci.* **28**, 1539 (2003). doi: 10.1016/j.progpolymsci.2003.08.002

75. R. F. Frindt, D. Yang, P. Westreich, Exfoliated single molecular layers of $Mn_{0.8}PS_3$ and $Cd_{0.8}PS_3$. *J. Mater. Res.* **20**, 1107 (2005). doi: 10.1557/JMR.2005.0161

76. J. Heising, M. G. Kanatzidis, Structure of restacked MoS_2 and WS_2 elucidated by electron crystallography. *J. Am. Chem. Soc.* **121**, 638 (1999). doi: 10.1021/ja983043c

77. S. Pavlidou, C. D. Papaspyrides, A review on polymer–layered silicate nanocomposites. *Prog. Polym. Sci.* **33**, 1119 (2008). doi: 10.1016/j.progpolymsci.2008.07.008

78. S. Stankovich et al., Graphene-based composite materials. *Nature* **442**, 282 (2006). doi: 10.1038/nature04969; pmid: 16855586

79. H. D. Huang et al., High barrier graphene oxide nanosheet/poly(vinyl alcohol) nanocomposite films. *J. Membr. Sci.* **409**, 156 (2012). doi: 10.1016/j.memsci.2012.03.051

80. U. Khan et al., Polymer reinforcement using liquid-exfoliated boron nitride nanosheets. *Nanoscale* **5**, 581 (2013). doi: 10.1039/c2nr33049k; pmid: 23203296

81. G. Cunningham et al., Percolation scaling in composites of exfoliated MoS_2 filled with nanotubes and graphene. *Nanoscale* **4**, 6260 (2012). doi: 10.1039/c2nr31782f; pmid: 22961125

82. Y. W. Zhu et al., Carbon-based supercapacitors produced by activation of graphene. *Science* **332**, 1537 (2011). doi: 10.1126/science.1200770; pmid: 21566159

83. A. B. Laursen, S. Kegnaes, S. Dahl, I. Chorkendorff, *Energy Environ. Sci.* **5**, 5577 (2012).

84. A. Kudo, Y. Miseki, Heterogeneous photocatalyst materials for water splitting. *Chem. Soc. Rev.* **38**, 253 (2009). doi: 10.1039/b800489g; pmid: 19088977

85. J. Pu et al., Highly flexible MoS_2 thin-film transistors with ion gel dielectrics. *Nano Lett.* **12**, 4013 (2012). doi: 10.1021/nl301335q; pmid: 22799885

86. K. S. Novoselov, A. H. C. Neto, Two-dimensional crystals-based heterostructures: Materials with tailored properties. *Phys. Scr.* **T146**, 014006 (2012). doi: 10.1088/0031-8949/2012/T146/014006

87. Z. Y. Yin et al., Single-layer MoS_2 phototransistors. *ACS Nano* **6**, 74 (2012). doi: 10.1021/nn2024557; pmid: 22165908

88. S. Park, R. S. Ruoff, Chemical methods for the production of graphenes. *Nat. Nanotechnol.* **4**, 217 (2009). doi: 10.1038/nnano.2009.58; pmid: 19350030

89. M. J. Allen, V. C. Tung, R. B. Kaner, Honeycomb carbon: A review of graphene. *Chem. Rev.* **110**, 132 (2010). doi: 10.1021/cr900070d; pmid: 19610631

90. C. R. Dean et al., Boron nitride substrates for high-quality graphene electronics. *Nat. Nanotechnol.* **5**, 722 (2010). doi: 10.1038/nnano.2010.172; pmid: 20729834

91. A. S. Golub, Y. V. Zubavichus, Y. L. Slovokhotov, Y. N. Nikovikov, Single-layer dispersions of transition metal dichalcogenides in the synthesis of intercalation compounds. *Usp. Khim.* **72**, 123 (2003). doi: 10.1070/RC2003v072n02ABEH000789

92. B. Radisavljevic, A. Radenovic, J. Brivio, V. Giacometti, A. Kis, Single-layer MoS_2 transistors. *Nat. Nanotechnol.* **6**, 147 (2011). doi: 10.1038/nnano.2010.279; pmid: 21278752

93. H. S. Lee et al., MoS_2 nanosheet phototransistors with thickness-modulated optical energy gap. *Nano Lett.* **12**, 3695 (2012). doi: 10.1021/nl301485q; pmid: 22681413

94. H. L. Tsai, J. L. Schindler, C. R. Kannewurf, M. G. Kanatzidis, Plastic superconducting polymer–$NbSe_2$ nanocomposites. *Chem. Mater.* **9**, 875 (1997). doi: 10.1021/cm960516a

95. F. A. Levy, *Physics and Chemistry of Layered Materials, vol. 6, Intercalated Layered Materials* (D. Reidel Publishing Company, Dordrecht, Netherlands, 1979).

96. Y. Onuki, R. Inada, S. Tanuma, S. Yamanaka, H. Kamimura, Electrochemical characteristics of transition-metal trichalcogenides in the secondary lithium battery. *Solid State Ion.* **11**, 195 (1983). doi: 10.1016/0167-2738(83)90024-3

97. P. J. S. Foot, J. Suradi, P. A. Lee, Optical and electronic properties of the layered semiconductors $NiPS_3$ and $FePS_3$. *Mater. Res. Bull.* **15**, 189 (1980). doi: 10.1016/0025-5408(80)90118-X

98. Y. Takano et al., Magnetic properties and specific heat of MPS3 (M=Mn, Fe, Zn). *J. Magn. Magn. Mater.* **272**, E593 (2004). doi: 10.1016/j.jmmm.2003.12.621

99. L. Wang, P. Brazis, M. Rocci, C. R. Kannewurf, M. G. Kanatzidis, A new redox host for intercalative polymerization: Insertion of polyaniline into α-$RuCl_3$. *Chem. Mater.* **10**, 3298 (1998). doi: 10.1021/cm980474l

100. N. Preda, L. Mihut, M. Baibarac, I. Baltog, *Acta Physica Polonica A* **116**, 81 (2009).

101. M. Kryszewski, Nanointercalates—novel class of materials with promising properties. *Synth. Met.* **109**, 47 (2000). doi: 10.1016/S0379-6779(99)00197-6

102. T. Sasaki, M. Watanabe, H. Hashizume, H. Yamada, H. Nakazawa, Pairwise association of nanosheets and dynamic reassembling process initiated from it macromolecule-like aspects for a colloidal suspension of an exfoliated titanate. *J. Am. Chem. Soc.* **118**, 8329 (1996). doi: 10.1021/ja960073b

103. Z. Liu, K. Ooi, H. Kanoh, W. Tang, T. Tomida, Swelling and delamination behaviors of birnessite-type manganese oxide by intercalation of tetraalkylammonium ions. *Langmuir* **16**, 4154 (2000). doi: 10.1021/la9913755

104. A. Takagaki et al., Exfoliated HNb_3O_8 nanosheets as a strong protonic solid acid. *Chem. Mater.* **17**, 2487 (2005). doi: 10.1021/cm047990y

105. Y. P. Chen et al., Polyaniline-intercalated layered vanadium oxide nanocomposites—One-pot hydrothermal synthesis and application in lithium battery. *Nanoscale* **2**, 2131 (2010). doi: 10.1039/c0nr00246a; pmid: 20835437

106. Y. Qian, S. B. Lu, F. L. Gao, Preparation of MnO_2/graphene composite as electrode material for supercapacitors. *J. Mater. Sci.* **46**, 3517 (2011). doi: 10.1007/s10853-011-5260-y

107. J. H. Liu, J. S. Chen, X. F. Wei, X. W. Lou, X. W. Liu, Sandwich-like, stacked ultrathin titanate nanosheets for ultrafast lithium storage. *Adv. Mater.* **23**, 998 (2011). doi: 10.1002/adma.201003759; pmid: 21341313

108. A. Takagaki, C. Tagusagawa, S. Hayashi, M. Hara, K. Domen, *Energy Environ. Sci.* **3**, 82 (2010).

109. M. Osada et al., Controlled polarizability of one-nanometer-thick oxide nanosheets for tailored, high-κ nanodielectrics. *Adv. Funct. Mater.* **21**, 3482 (2011). doi: 10.1002/adfm.201100580

110. H. Tagaya, K. Ara, J. Kadokawa, M. Karasu, K. Chiba, Intercalation of organic compounds in the layered host lattice MoO_3. *J. Mater. Chem.* **4**, 551 (1994). doi: 10.1039/jm9940400551

111. A. V. Murugan, A. K. Viswanath, C. S. Gopinath, K. Vijayamohanan, Highly efficient organic-inorganic poly(3,4-ethylenedioxythiophene)-molybdenum trioxide nanocomposite electrodes for electrochemical supercapacitor. *J. Appl. Phys.* **100**, 074319 (2006). doi: 10.1063/1.2356788

112. C. G. Granqvist, Electrochromic tungsten oxide films: Review of progress 1993–1998. *Sol. Energy Mater. Sol. Cells* **60**, 201 (2000). doi: 10.1016/S0927-0248(99)00088-4

113. H. Kanno, R. J. Holmes, Y. Sun, S. Kena-Cohen, S. R. Forrest, White stacked electrophosphorescent organic light-emitting devices employing MoO_3 as a charge-generation layer. *Adv. Mater.* **18**, 339 (2006). doi: 10.1002/adma.200501915

114. R. E. Schaak, T. E. Mallouk, Exfoliation of layered rutile and perovskite tungstates. *Chem. Commun. (Camb.)* **7**, 706 (2002). doi: 10.1039/b110220f; pmid: 12119683

115. N. Miyamoto, S. Yamamoto, K. Shimasaki, K. Harada, Y. Yamauchi, Exfoliated nanosheets of layered perovskite $KCa_2Nb_3O_{10}$ as an inorganic liquid crystal. *Chem. Asian J.* **6**, 2936 (2011). doi: 10.1002/asia.201100279; pmid: 21786425

116. Y. Ebina, T. Sasaki, M. Watanabe, Study on exfoliation of layered perovskite-type niobates. *Solid State Ion.* **151**, 177 (2002). doi: 10.1016/S0167-2738(02)00707-5

117. M. M. J. Treacy, M. E. Fisher, A. J. Jacobson, *Philos. Mag.* **72**, 161 (1995).

118. C. A. P. de Araujo, J. D. Cuchiaro, L. D. McMillan, M. C. Scott, J. F. Scott, Fatigue-free ferroelectric capacitors with platinum electrodes. *Nature* **374**, 627 (1995). doi: 10.1038/374627a0

119. S. K. Deb, Optical and photoelectric properties and colour centres in thin films of tungsten oxide. *Philos. Mag.* **27**, 801 (1973). doi: 10.1080/14786437308227562

120. S. Ida et al., Preparation of a blue luminescent nanosheet derived from layered perovskite $Bi_2SrTa_2O_9$. *J. Am. Chem. Soc.* **129**, 8956 (2007). doi: 10.1021/ja073105b; pmid: 17602633

121. S. J. Clarke et al., Structures, physical properties, and chemistry of layered oxychalcogenides and oxypnictides. *Inorg. Chem.* **47**, 8473 (2008). doi: 10.1021/ic8009964; pmid: 18821814

122. R. H. Herber, Y. Maeda, Intercalation compounds of iron(III) oxychloride: Systematics of nitrogen-containing Lewis base intercalants. *Inorg. Chem.* **20**, 1409 (1981). doi: 10.1021/ic50219a016

123. K. Kanamura, H. Sakaebe, C. Zhen, Z. Takehara, Application of FeOCl derivative for a secondary lithium battery. *J. Electrochem. Soc.* **138**, 2971 (1991). doi: 10.1149/1.2085350

124. V. K. Lukyanyuk, Z. D. Kovalyuk, Sodium intercalation into indium and gallium selenides. *Phys. Status Solidi, A Appl. Res.* **102**, K1 (1987). doi: 10.1002/pssa.2211020148

125. N. Mirabal, V. Lavayen, E. Benavente, M. A. Santa Ana, G. Gonzalez, Synthesis, functionalization, and properties of intercalation compounds. *Microelectron. J.* **35**, 37 (2004). doi: 10.1016/S0026-2692(03)00220-9

126. A. Bourdon, E. Bringuier, M. T. Portella, M. Vivières, N. Piccioli, Angular properties of second-harmonic polarization due to high-order nonlinearities: Application to GaSe and InSe. *Phys. Rev. Lett.* **65**, 1925 (1990). doi: 10.1103/PhysRevLett.65.1925; pmid: 10042399

127. A. Bhambhani, C. V. Kumar, Enzyme-inorganic nanoporous materials: Stabilization of proteins intercalated in α-zirconium(IV) phosphate by a denaturant. *Microporous Mesoporous Mater.* **110**, 517 (2008). doi: 10.1016/j.micromeso.2007.06.050

128. G. Alberti, C. Dionigi, E. Giontella, S. MurciaMascaros, R. Vivani. *J. Colloid Interface Sci.* **188**, 27 (1997). doi: 10.1006/jcis.1996.4679

129. P. Atienzar *et al.*, *Energy Environ. Sci.* **4**, 4718 (2011).

130. T. J. Pinnavaia, Intercalated clay catalysts. *Science* **220**, 365 (1983). doi: 10.1126/science.220.4595.365 pmid: 17831398

131. S. M. Auerbach, K. A. Carrado, P. K. Dutta, Eds., *Handbook of Layered Materials* (Marcel Dekker, New York, 2004).

132. S. K. Srivastava, I. P. Singh, Hybrid epoxy nanocomposites: Lightweight materials for structural applications. *Polym. J.* **44**, 334 (2012). doi: 10.1038/pj.2011.140

133. A. Arora, V. Choudhary, D. K. Sharma, Effect of clay content and clay/surfactant on the mechanical, thermal and barrier properties of polystyrene/organoclay nanocomposites. *J. Polym. Res.* **18**, 843 (2011). doi: 10.1007/s10965-010-9481-6

134. M. Chakraborti, J. K. Jackson, D. Plackett, D. M. Brunette, H. M. Burt, Drug intercalation in layered double hydroxide clay: Application in the development of a nanocomposite film for guided tissue regeneration. *Int. J. Pharm.* **416**, 305 (2011). pmid: 21708236

135. N. Nhlapo, T. Motumi, E. Landman, S. M. C. Verryn, W. W. Focke, Surfactant-assisted fatty acid intercalation of layered double hydroxides. *J. Mater. Sci.* **43**, 1033 (2008). doi: 10.1007/s10853-007-2251-0

136. L. Moyo, W. W. Focke, F. Labuschagne, S. Verryn, Layered double hydroxide intercalated with sodium dodecyl sulfate. *Molecular Crystals and Liquid Crystals* **555**, 51 (2012). doi: 10.1080/15421406.2012.634366

137. Q. L. Wu *et al.*, Characterization of exfoliated layered double hydroxide (LDH, Mg/Al = 3) nanosheets at high concentrations in formamide. *J. Mater. Chem.* **17**, 965 (2007). doi: 10.1039/b612389a

138. J. Y. Miao, M. Xue, H. Itoh, Q. Feng, Hydrothermal synthesis of layered hydroxide zinc benzoate compounds and their exfoliation reactions. *J. Mater. Chem.* **16**, 474 (2006). doi: 10.1039/b511110b

139. M. Darder, P. Aranda, A. I. Ruiz, F. M. Fernandes, E. Ruiz-Hitzky, Design and preparation of bionanocomposites based on layered solids with functional and structural properties. *Mater. Sci. Technol.* **24**, 1100 (2008). doi: 10.1179/174328408X341780

140. M. Naguib *et al.*, MXene: A promising transition metal carbide anode for lithium-ion batteries. *Electrochem. Commun.* **16**, 61 (2012). doi: 10.1016/j.elecom.2012.01.002